Investigating the possibility of a bottom-heavy IMF in giant ellipticals

Using the CO index to constrain the Initial Mass Funcion for giant ellipticals

U. Christoffer Fremling

Department of Astronomy, Stockholm University

SE-106 91 Stockholm, Sweden

Supervised by: Erik Zackrisson

June 10, 2011

ABSTRACT

Recent observations have hinted at the possibility of a bottom-heavy Initial Mass Function (IMF) in elliptical galaxies. The aims of this project is to determine if the CO bandhead at 2.3 μm can be used to constrain the IMF in giant ellipticals, and to determine if there is evidence for bottom-heavy IMFs in giant elliptical galaxies in currently available observational CO index data.

A Stellar Population Synthesis (SPS) model is used to calculate theoretical galaxy spectra including the CO bandhead. Several CO index definitions are used to analyze the theoretical spectra and an attempt at validating the results, by comparing the SPS model output with observational data, is also made. According to the current publicly available SPS model PEGASE-HR it is shown that constraining the IMF using the CO index appears promising. However, it is also shown that the theoretical stellar atmosphere grid that is used in PEGASE-HR may not be sufficiently accurate in the CO region. An attempt at calibrating the model is made, but a new stellar population model, based on empirical stellar spectra in the region of the CO index at 2.3 μm would need to be constructed to address this issue properly.

We also note that observed mass-to-light (M/L) ratios for at least some of the giant ellipticals that have been argued to exhibit evidence for a bottom-heavy IMF, in fact appear to be too low to be consistent with synthetic SPS model M/L ratios for very bottom-heavy scenarios.

Subject headings: Galaxies: formation - Galaxies: evolution - Galaxies: stellar content - Galaxies: star formation - Galaxies: elliptical and lenticular, cD

Contents

List of Tables

1.   Introduction

According to the theory of stellar structure and evolution (see Iben 1991, for a review) the main parameter deciding the life and evolution of a star is it's mass. Thus, the initial properties of galaxies and their subsequent evolution will be determined by the initial distribution of the stellar masses. This initial distribution is traditionally described by a mathematical function, the Initial Mass Function (IMF). Most current theories of star formation assume that the IMF is universal. However, In the recent paper by van Dokkum & Conroy (2010) it is proposed that there is a large population of low mass stars in luminous ellipticals not compatible with a universal IMF, and that the IMF instead depends on the prevailing physical conditions as the galaxies are formed. If this is indeed the case, it is of critical importance to our understanding of star and galaxy formation.

The Initial Mass Function was originally introduced by Edwin Salpeter (Salpeter 1955) as a power law of the form:

$$\Phi(\log m) = \mathrm{d}N/\mathrm{d}\log m \propto m^{-\Gamma}, \tag{1}$$

where Γ is a constant, m is the mass of a star and N is the number of stars in the logarithmic mass range $\log m + \mathrm{d}\log m$. Eq. (1) allows us to find the amount of stars in a logarithmic mass interval by integration. Initial Mass Functions of this form are commonly referred to as "Salpeter-like IMFs". The value for Γ that Salpeter found was, Γ=1.35, and this has later been labeled the "Salpeter slope". In van Dokkum & Conroy (2010) it is found that the best fitting IMF for the luminous ellipticals included in the study is given by a Salpeter-like IMF with Γ=2.0. IMFs with Γ>1.35 are commonly referred to as bottom-heavy IMFs, and in such a bottom-heavy scenario Eq. (1) results in an initial distribution with more emphasis on lower mass stars. The notation used above is identical to the notation in the recent IMF review paper by Jeffery (2010), containing an update on current IMF research.

Since Salpeter's 1955 paper It should however be mentioned that there has been substantial development of the functional form of the IMF. During the 1970s it became apparent that the slope of the IMF appears to change for smaller masses, hence the IMF cannot be completely described by a single power-law. In Miller & Scalo (1979) a log-normal form of the IMF was suggested and later in Kroupa et al. (1993), a multi-segmented power-law was proposed. Kroupa's multi-segmented approach is further refined in Kroupa (2002). IMFs of this form are also commonly referred to as "Kroupa IMFs". The IMF proposed in Kroupa (2002) is still commonly used, and it is noteworthy that for masses above 0.5 $M_\odot$ the slope is very similar to the Salpeter slope; thus the Salpeter IMF remains a good benchmark for IMF research. This is also why I have chosen, similarly to van Dokkum & Conroy (2010), to mainly work with Salpeter-like IMFs in this paper.

As already mentioned, the Salpeter IMF and it's subsequent variations play a central role in star formation theory, as any valid theory needs to be able to explain the distribution of the initial stellar masses during galaxy formation: the IMF (see McKee & Ostriker 2007, for a review of current star formation theory). However, the main goal of this paper is to investigate if the results obtained by van Dokkum & Conroy (2010) can be validated using a Stellar Population Synthesis (SPS) model to calculate synthetic galaxy spectra for elliptical galaxies. In Section 3 the publicly

available SPS model PEGASE-HR (Le Borgne et al. 2004) is briefly described along with how it has been used for this project. In Section 4, model galaxy spectra around the CO bandhead at 2.3 μm are shown to exhibit a similar behavior to what is shown by Mieske & Kroupa (2008); a higher abundance of low mass stars–i.e. a bottom heavy IMF–results in a shallower CO bandhead. In Section 4 the other main factors affecting the shape of the CO bandhead are also discussed: the initial metallicity, the age of the galaxy and possible remaining star formation. In Section 5, we look at two index definitions for analyzing CO absorption, the CO and the D_{CO} index. In Section 6 we present the results of the spectral synthesis; we investigate the time evolution of the CO indices for the model spectra while accounting for the most likely metallicity and star formation scenarios. In Section 6, we also attempt to investigate if the change in the CO and D_{CO} indices as a result of a bottom-heavy IMF, as proposed by van Dokkum & Conroy (2010), with $\Gamma = 2.0$ is big enough to constrain the IMF in giant elliptical galaxies by looking at the spread in the calculated CO and D_{CO} index values from the SPS models. In Section 6.1 we compare our models with currently available observational CO and D_{CO} data. This is also where some problems appear, which leads us to Section 7, where the accuracy at the CO bandhead of the stellar population model PEGASE and the stellar library BaSeL (Lejeune et al. 1997, 1998) is investigated. Possible solutions to the problem with the BaSeL library are also discussed. In Section 8 we present some additional PEGASE-HR output, namely the mass-to-light ratio and the V-I_C color index for the different IMFs. In Section 9, we discuss the general results and implications of this project and take a look at what needs to be done to arrive at more reliable conclusions.

2. Giant elliptical galaxies

For most of this project we will be working with models of elliptical and giant elliptical galaxies, so it is logical to start with a brief introduction to these objects. The largest elliptical galaxies, the giant ellipticals, have stellar masses $M_* > 10^{11} M_\odot$ (Raichoor et al. 2011; Bernardi et al. 2010; Bolton et al. 2008), and these will be of particular interest for this project. The details on how elliptical galaxies formed is still an open question, but age estimates (Yamada 2004) tell us that they are very old (> 10 Gyr, for the most massive galaxies). Since they usually contain little gas, and have very low star formation (Sandage 1986; Grebel 2011; Knapp 1999), the classical approach is to assume that they formed at an early epoch of the universe in a short (< 1 Gyr) intense period of star formation that consumed the majority of the interstellar gas. However, even though we will be using the classical approach in this project, it is not really considered an entirely realistic scenario anymore. The very recent paper by McDermid et al. (2011) still concludes that the overwhelming majority of the stellar mass in early-type galaxies formed at early epochs, so there has not been a major change in our understanding, however, in De Lucia et al. (2006) data from the *Millenium Simulation* is used to show that a typical elliptical galaxy form from the merger of two comparably sized or several smaller progenitor galaxies. The most massive giant ellipticals are shown to form from up to 5 comparably sized progenitor galaxies. Further support for the merger scenario can be found in Kormendy et al. (2009). On the nature of the progenitors: in Naab & Burkert (2001) it

is shown that collisionless N-body simulations of merging disk galaxies result in simulated photo-metric and kinematic properties that are in good agreement with the properties of observed giant ellipticals. So, an arguably more realistic hyphothesis is that the most massive ellipticals formed in mergers of several disk galaxies. Additionally, in Kaviraj et al. (2009) evidence for recent smaller mergers in early-type galaxies is presented. This would mean that in reality there will be several different stellar populations in a giant elliptical galaxy originating from the various progenitors. However, regardless of the more minute details of the formation, the classical scenario is still a good approximation: models of elliptical galaxies using a single stellar population formed in an instantaneous brust have been shown to be in good agreement with observations (Fioc & Rocca-Volmerange 1997; Kotulla et al. 2009; Vazdekis et al. 2010; Rogers et al. 2010).

So far we have only considered the stellar masses of giant ellipticals. However, the *Millenium Simulation* merger scenario investigated by De Lucia et al. (2006) relies on the ΛCDM model of the universe, so it is assumed that dark matter (DM) comprises 23% of the energy density budget of the universe. Thus it is natural to expect elliptical galaxies to also contain DM. The need for DM in many elliptical galaxies has finally been firmly established by Buote & Humphrey (2011) with the help of X-ray mass-to-light ratio data from *Chandra* and *XMM*. In Section 8.1 we will present theoretical stellar M/L ratio calculations for different initial mass functions.

3. The Stellar Population Synthesis model

For the evolutionary synthesis of galaxies for this project the publicly available stellar population synthesis model PEGASE-HR (Le Borgne et al. 2004) has been used. This is an updated version of PEGASE-2 (Fioc & Rocca-Volmerange 1997, 1999). PEGASE-HR includes a high resolution stellar library that has not been used for this paper as it is restricted to wavelengths in the visible range. Instead the somewhat older BaSeL library by Lejeune et al. (1997, 1998) has been used as it allows generation of synthetic spectra around the CO bandhead. The motivation for using PEGASE-HR over PEGASE.2 is purely practical. PEGASE-HR contains an updated interface that allows for somewhat simpler operation.

For more details about the workings of SPS modeling, I refer to the articles related to PEGASE-HR/PEGASE.2 above, especially Fioc & Rocca-Volmerange (1997), but the fundamentals of evo-lutionary synthesis of galaxies important for this paper are fortunately quite simple: If we begin by picturing a Single Stellar Population[1] (SSP), which is the simplest evolutionary scenario, the IMF will initially have determined the distribution of the stellar masses. The time evolution of the stars are then decided by theoretical evolutionary tracks (In PEGASE mainly from the "Padova" group). This means that at any given time the effective temperature, luminosity and surface gravity of all the stars in the galaxy will be known. If we are interested in synthetic spectra, which is the

---

[1]SSP: A population consisting of stars born at the same time with the same initial element composition. An SSP is also sometimes called an instantaneous burst stellar population.

case for most of this paper, the model can then match the stars in the galaxy to theoretical stellar atmosphere spectra from the stellar library and synthesize all the relevant spectra into an integrated galaxy spectum. However, PEGASE-HR is also capable of working with composite stellar populations, CSPs, which can for example be evolutionary scenarios where the stars in the modeled galaxy form during an extended period of time, or during several short bursts of star formation at different times during the life of the galaxy. We will be utilizing both types of models in this project. Additionally, PEGASE does not only calculate synthetic spectra, it can also output the time evolution of the mass in stars, the mass in gas, the mass in white dwarfs, various color indices, etc. For a complete listing I refer to the PEGASE documentation (Fioc & Rocca-Volmerange 1997). For most of this project we will be working with analyzing synthetic spectra, but in Section 8.1 we present some of this additional output from PEGASE-HR, namely the mass-to-light ratio and the V-I_C color-index for different IMFs.

All the input parameters used when running PEGASE-HR have been left at their default values unless a change is explicitly stated. The parameters that are subject to modification are: the IMF, the initial metallicity of the gas and the star formation scenario. In Table 1, a complete list of all the modified parameters for all models that are included in this paper can be found. We will henceforth refer to the different models by mentioning the main identifying parameter value(s), such as the slope of the IMF and the metallicity, or simply the model number. It is however, always possible to check Table 1 to obtain the full listing of the modified parameter values used in any particular model variation. The output from PEGASE-HR was converted from .fits to .dat using the simple conversion-application included in PEGASE-HR. The .dat files were then imported into matlab and analyzed. Example code that can be used for importing and analyzing the .dat files is found in appendix A.

4. CO absorption in giant ellipticals

In this section we will look closer at the major factors influencing CO absorption in giant ellipticals: the IMF, the age of the galaxy, the star formation history and the metallicity. We mainly focus on the galaxies included in van Dokkum & Conroy (2010). Compiled data for these can be found in Table 2. The aim is to determine how to account for each of the major factors in our evolutionary synthesis modeling; what parameter values should be used during the modeling to obtain a set of models representing a realistic scenario. The effect of the IMF on the CO absorption is investigated with the help of initial assumptions for the parameters in Section 4.1. In sections 4.2, 4.3, 4.4 we use currently available observational and theoretical results to obtain good estimates, with errors where applicable, for the age, the star formation rate and the metallicity in giant elliptical galaxies. The net result will be that we obtain a set of models (Table 1) representing a scenario with a slightly bigger spread in observational parameters than the best current observational data. The compiled results from the models will be investigated in Section 6.
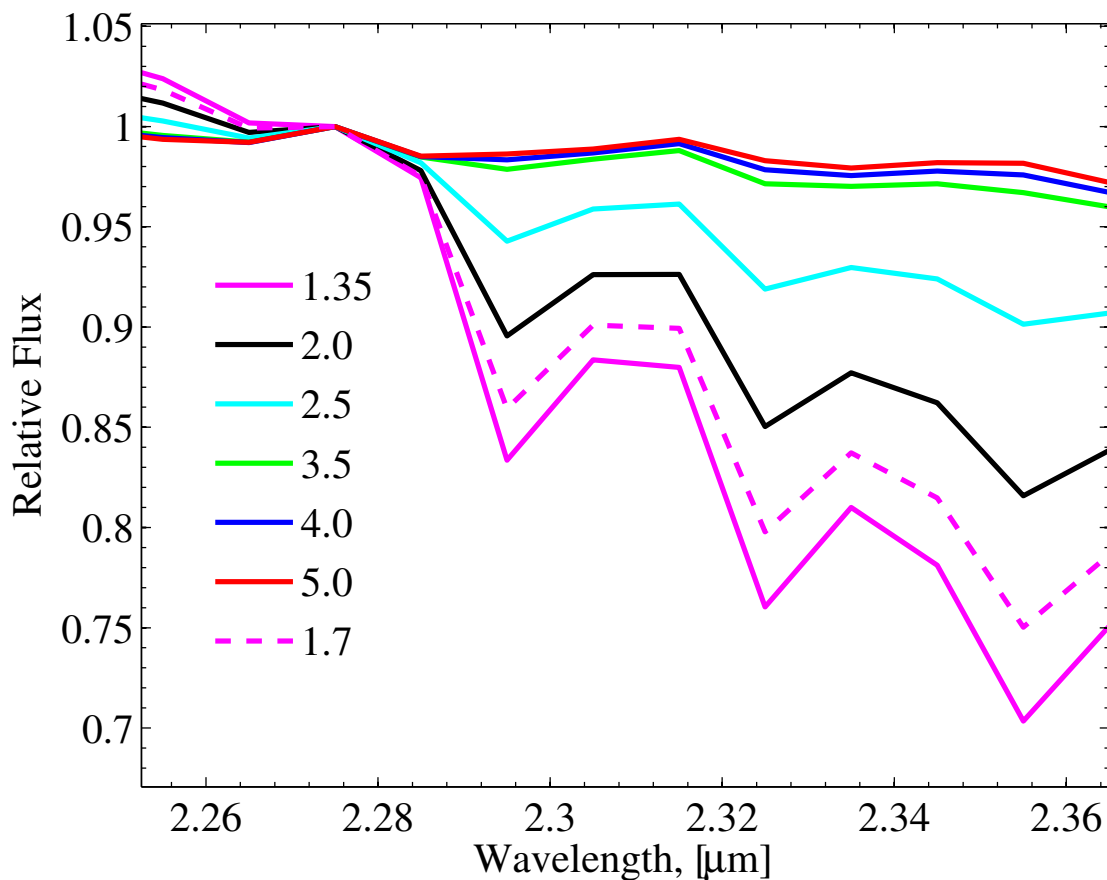
Fig. 1.— Synthetic spectra around the CO region at 2.3 μm generated by PEGASE-HR. The lines represent the synthetic galaxy spectra at age = 10 Gyr for different IMFs with values for Γ ranging from the Salpeter value $\Gamma=1.35$ to an extremely bottom-heavy IMF with $\Gamma=5.0$. All of the models were calculated assuming roughly solar metallicity (Z=0.02) and an instanataneous-burst star formation scenario. All spectra have been normalized at 2.275 μm. Models 1,7 and 14-18 have been used. Check Table 1 for a complete list of the parameters used in the models while running PEGASE-HR.

4.1. IMF

Evidence for a bottom-heavy IMF (Γ = 2.0) in elliptical galaxies[1] can be found in van Dokkum & Conroy (2010), where direct detection of the light from low mass stars (M<0.3M$_\odot$) is shown. The direct detection of the light from low mass stars implies, according to van Dokkum & Conroy (2010), that they are very abundant in elliptical galaxies. As late-type low mass stars have a much lower CO absorption than late-type giant stars (Frogel et al. 1978), it seems logical that a high abundance of low mass stars would have an effect on the total CO absorption of a galaxy. In Kroupa & Gilmore (1994) it is indeed shown that CO absorption appears to be promising for the purpose of detecting large populations of low mass stars, and more recently, in Mieske & Kroupa (2008), it is addittionally concluded that measuring the CO absorption around 2.35 μm appears promising as a tool for constraining the low-mass slope of the IMF in extragalactic systems.

As we can see, there is a substantial amount of earlier work warranting closer investigation of the effect of the IMF on the CO region; this is also the main goal of this paper. Synthetic spectra for SSPs with increasingly bottom-heavy IMFs are displayed in Figure 1, showing a clear negative correlation between increasing Γ and the CO absorption in the synthetic spectra generated by PEGASE-HR. A more bottom-heavy IMF results in less CO absorption. For the generation of the synthetic spectra in Figure 1, we have used standard initial assumptions for the model parameters; Z=Z$_\odot$ (solar metallicity, here assumed to be Z=0.020), an SSP for the star formation scenario, and age 10 Gyr for the age. All of these parameters need to be investigated more closely if we aim to create realistic models of elliptical galaxies. However, we have clearly shown in Fig. 1 that the IMF does effect the strength of CO absorption at 2.3 μm. For the rest of this paper the IMFs of interest will be the regular Salpeter IMF with Γ = 1.35 and the best-fit IMF proposed by van Dokkum & Conroy (2010) with Γ = 2.0. Using simple percentage calculation and the same normalization as in Figure 1 the effect when changing from Γ = 1.35 to Γ = 2.0 on the depth of the first CO feature is on the order of 7%. However, this value is clearly dependent on the choice of normalization, and a better method for analyzing the CO wavelength range is needed. This will be discussed in Section 5. However, before we can move on to any more in-depth analysis of the synthetic spectra, other major factors influencing the CO absorption of a galaxy should also be discussed.

4.2. Age

As a galaxy evolves in time the distribution of the stellar masses will change; low mass stars live much longer than giant stars, and as already discussed above (Kroupa & Gilmore 1994) the distribution of stellar masses directly influence the CO absorption. This distribution can be thought

---

[1]The galaxies included in the IMF study by van Dokkum & Conroy (2010) are NGC 4261, NGC 4374, NGC 4472, NGC 4649 in the Virgo cluster and NGC 4840, NGC 4926, IC 3976, NGC 4889 in the Coma cluster (see Table 2).

of as the Mass Function (MF) of the galaxy, the MF changes with time as the stars in the galaxy evolve along their evolutionary tracks and it is of course a direct result of the Initial Mass Function. The MF at the present day is usually called the current mass funtion. In Figure 1 we can see that the IMF directly affects the distribution of stellar masses (the MF) at age = 10 Gyr. Essentially this just means that if we aim to compare CO absorption in synthetic spectra and in spectra from observed galaxies, we will have to account for the age of the galaxies. PEGASE-HR automatically calculates the synthetic data and spectra in 68 steps for ages in the range 1 Myr - 20 Gyr, i.e. it is always simple to look at the entire time evolution for any interesting property. What remains then is only to investigate the synthetic spectra corresponing to the correct age interval. There is some controversy about the ages of elliptical galaxies, as accurate measurements are difficult, but for example in Yamada (2004) it is found that massive elliptical galaxies in the Virgo cluster have an uniformly old age (>10 Gyr), thus, if we aim to look at an average giant elliptical galaxy, a reasonable age interval for closer investigation of the modeled spectra would be 10 Gyr to the current age of the universe. In Table 2 age data by Terlevich & Forbes (2002), Annibali et al. (2007), or Sánchez-Blázquez et al. (2006) for most of the galaxies studied by van Dokkum & Conroy (2010) can be found. The ages for the galaxies in Table 2 confirm that the above choice of interval is reasonable; for the galaxies with available data in the three references above the mean value for the age is 11 Gyr. However, as mentioned above, accurate measurements are difficult, the errors in the ages that are most relevant to this paper from Terlevich & Forbes (2002) are large, but at least less than ±20%, and are in fact shown not to be a problem in Section 6.

4.3. Star formation history

Another major factor influencing the CO absorption is how the stars in a galaxy have formed: the history of the star formation rate. The star formation rate directly influences the MF for any given time in the history of a galaxy: if all the stars formed a long time ago the current MF will look very different from a scenario where there are still new stars forming, as this means that there will still be very massive stars, even in an old galaxy. As discussed in Section 3 the simplest scenario is a single stellar population, i.e. all the stars in the galaxy are assumed to have formed instantly at some specific time. In e.g. Grebel (2011) it is concluded that in very massive elliptical galaxies the stars form rapidly during a very short period of time early in the life of the galaxy. So an SSP should be reasonable as an initial approximation for the SFR for the luminous elliptical galaxies relevant to this project (Table 2). In an SSP model, it is additionally easy to follow all the significant events in the evolution of a galaxy, as there will be no smoothing of the spectra due to formation of new stars. However, it is of course not entirely realistic to assume that all the gas in the galaxy at some point instantly turned into stars. The currently preferred approach (Kotulla et al. (2009), Kennicutt (1998), Sandage (1986)) when modeling elliptical galaxies is to work with an exponentially declining SFR of the form:

$$SFR(t) = \frac{p_2}{p_1} \exp(-\frac{t}{p_1}), \tag{2}$$

where p_1 is a constant, given in Myr, that sets the duration of the star formation and p_2 is a constant, given in $M_\odot$, that scales the absolute initial rate of the star formation. So to account for the fact that SSPs might not be entirely realistic for modeling elliptical galaxies we chose to run models for both instantaneous burst (SSP) and exponentially declining star formation of 1Gyr duration. Table 1 contains the values of p_1 and p_2 that has been used in PEGASE-HR.

4.4. Metallicity

A clear correlation between the CO index and the metallicity is observationally shown in Frogel et al. (2001) and a similar dependence can be found by inspecting the theoretical spectra included in the BaSeL library (Lejeune et al. 1998). So, another major factor influencing the CO absorption of a galaxy is of course the possibility for varying metallicity in the gas from where the stars are initially formed. If the metallicity is low there will be less CO that can contribute to the absorption and vice versa. Naturally there will also be a time evolution of the metallicity of the galaxy; the interstellar gas is enriched by evolving stars: stellar winds, supernovae, etc., and stars that form from the enriched ISM will have a higher metallicity. This means that, if we are working with a galaxy with an exponentially declining star formation rate, the metalicity of the stars is a function of the age and the initial metallicity of the gas. However, for an SSP the initial metallicity of the stars will be the same for the entire life of the galaxy and only depend on the metallicity of the gas. In Table 2 metallicity (mass fraction, Z) data from Annibali et al. (2007) and $[Fe/H]$ metallicity values from Terlevich & Forbes (2002) can be found, when avalable, for the galaxies studied by van Dokkum & Conroy (2010). The error in the measurements of the metallicity by Terlevich & Forbes (2002) is $\pm$ 0.1 dex. When accounting for this error we can see that in Table 2 three of the galaxies (NGC 4261, NGC 4374, NGC4926) are relatively compatible with a solar metallicity model, and the remaining three with available data (NGC4472, NGC 4649 NGC, 4840) have a higher metallicity. With the error ($\pm$0.1dex) in the metallicity measurements by Terlevich & Forbes (2002) in mind, we have chosen to work with a set of models centered around solar metallicity ($[Fe/H] = 0.0$), which in the heavy mass fraction Z used as the input parameter in PEGASE-HR, roughly correspond to models with Z=0.02, Z=0.016 and Z=0.024. Here we have used the, arguably somewhat dated[1], assumption that the solar metallicity mass fraction, Z, corresponding to $[Fe/H] = 0$ is given by $Z = 0.02$. The same initial metallicity has been used in both the exponentially declining star formation and the SSP models. In practice this means, when combining both SSP and SFR models, the spread in the CO absorption due to the metallicity intervals used will be sligthly higher than what would be expected for a $\pm$ 0.1 dex interval as the metallicity actually increases with age for the models with star formation, shifting them towars higher CO absorption. In Section 6 it is found, when looking at the results of the models, that this does not pose a problem. Subsequently, no attempt at calibration of the SSP and SFR model metallicities as a function of the galaxy age has been made.

---

[1]In e.g. (Asplund et al. 2004) arguments for a much lower solar metallicity, $Z_\odot$=0.013, are presented.
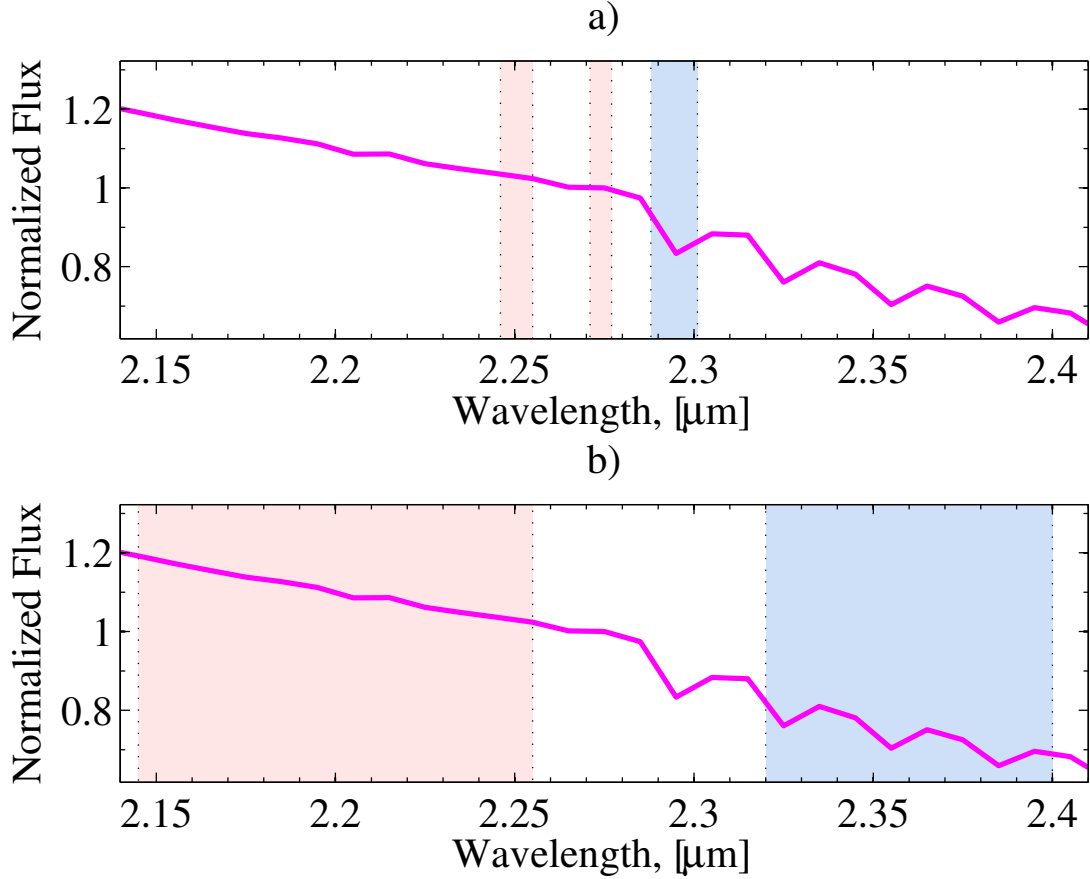
a)

b)

Fig. 2.— Integration intervals used in the CO index calculations. In a) we show the intervals for the D_{CO} index by Mármol-Queraltó et al. (2008). In b) we show the intervals for the CO_{KG} index defined by Kroupa & Gilmore (1994). The areas colored blue represent the absorption bands and the areas colored red represent the continuum bands. The magenta colored line represents the synthetic galaxy spectra generated by PEGASE-HR at age = 10 Gyr for a Salpeter IMF with solar metallicity (Z=0.02) and an instanataneous-burst star formation scenario. The spectrum has been normalized at 2.275 μm. Models 1 and 7 in Table 1 have been used.

5. The CO and D_{CO} indices

In Section 4 we have shown that there is a clear negative correlation between the IMF and the depth of the CO features around 2.35 μm in the synthetic spectra generated by PEGASE-HR. A rough estimate of the effect on the CO bandhead when going from a Salpeter IMF to a bottom-heavy IMF with $\Gamma = 2.0$ was estimated at around 7%. However, a better method for analyzing the CO bandhead is needed, and for this purpose I have chosen to use the traditional CO index as defined by Section 2.2 in Kroupa & Gilmore (1994) (hereafter K&G) along with the more modern CO index, the D_{CO} index as defined by Section 3.3 in Mármol-Queraltó et al. (2008). The K&G CO index (hereafter labeled CO_{KG}) is defined by:

$$CO_{KG} = -2.5 \log_{10} \left(\frac{\int_{2.320}^{2.400} f_\lambda \, d\lambda}{\int_{2.145}^{2.255} f_\lambda \, d\lambda} \right) - CO_0 \tag{3}$$

with the zero point $CO_0 = 0.564$ as calculated by K&G. The integration limits define the wavelength intervals in μm. The CO index in Eq. (3) essentially measures the equivalent width of the CO absorption band. The equivalent width allows a comparison of the strength of the CO absorption between the synthetic spectra without the need for normalization like in Section 4.

The D_{CO} index is similar to the CO_{KG} index but uses two intervals, $2.2460 \leq \lambda_{c_1}[\mu m] \leq 2.2550$ and $2.2710 \leq \lambda_{c_2}[\mu m] \leq 2.2770$ for measuring the continuum strength along with one interval, $2.2880 \leq \lambda_{a_1}[\mu m] \leq 2.3010$ for the CO absorption band. See Fig. 2 for an illustration of the continuum and absorption bands used in the CO_{KG} and D_{CO} index definitions. The D_{CO} index is measured as a generic discontinuity; the ratio between the average fluxes in the continuum and in the absorption bands, and it is defined by:

$$D_{CO} = \frac{\left(\frac{\int_{2.246}^{2.255} f_\lambda \, d\lambda + \int_{2.271}^{2.277} f_\lambda \, d\lambda}{\Delta\lambda_{c_1} + \Delta\lambda_{c_2}} \right)}{\left(\frac{\int_{2.288}^{2.301} f_\lambda \, d\lambda}{\Delta\lambda_{a_1}} \right)} \tag{4}$$

For a complete explanation and motivation for the choice of intervals in Eq. (4), we again refer to Mármol-Queraltó et al. (2008). The main point however, is that the D_{CO} index is less sensitive to spectral resolution, wavelength calibrations, signal-to-noise ratio and flux calibrations than previous index definitions.

The choice of working with the CO_{KG} index is mainly for legacy reasons, it allows direct comparison of the synthetic data from our models with photometric CO wavelength filter observations from Frogel et al. (1978) and previous synthetic CO_{KG} calculations by K&G. The choice of working with the D_{CO} index allows us to use a more modern tool to analyze the CO absorption, further allowing additional data-comparison to the much more recent CO absorption data by Mármol-Queraltó et al. (2009).

6.   Results from the spectral synthesis

In Figure 3 we can see the time evolution of the CO_{KG} index for the synthetic spectra generated by PEGASE-HR with all the major factors influencing the CO absorption discussed in Section 4 taken into account. In Figure 4 the CO_{KG} index is shown for age $10 - 14$ Gyr. In Figure 5 and 6, similar calculations for the D_{CO} index are displayed. In Figure 4 we can clearly see two groups of CO_{KG} index values centered around the Salpeter- and the bottom-heavy IMF-models with no star formation and solar metallicity. Note that there is next to no overlap of the CO_{KG} index values obtained from the two different IMFs. In Fig 6 we can see a similar behavior for the D_{CO} index data, albeit with a slightly larger overlap for the two IMFs. Also noteworthy in Figures 4 and 6 is that the impact of the age on the CO absorption and subsequently the CO indices is very small. Thus the large uncertainty (around 20%) in age determinations of giant ellipticals discussed in 4.4 does not really pose a problem. However, one factor we have not yet considered, is the errors that directly arise from the calculation of CO_{KG} and D_{CO} values from observed galaxy spectra. These errors do not originate from the factors discussed in Section 4. Instead they are a consequence of the index definition used and the quality of the observed galaxy spectra that the index calculation is applied to. In K&G there are unfortunately no errors specified, but for the D_{CO} index in Mármol-Queraltó et al. (2009) a procedure for calculating the error is given, and for all D_{CO} values presented there is also an explicitly given error, typically in the range 0.1% - 0.2%, and for the most accurate measurements $< 1\%$. The effect of a bottom-heavy IMF with $\Gamma = 2.0$ on the D_{CO} index is approximately 1.1% (percentage calculations on the center of the two IMF D_{CO} index ranges at age = 10 Gyr), so even this error seems to be sufficiently small. Under the assumption that the accuracy of eventual CO_{KG} measurements also can be made sufficiently small, Fig. 4 and Fig. 6 show that acording to synthetic spectra generated by PEGASE-HR in the age range $10 - 14$ Gyr, it at first glance appears fully possible to constrain the IMF using the CO indices as defined by K&G and by Mármol-Queraltó et al. (2008) . Currently there are no available CO_{KG} index mesurements for the interesting galaxies in van Dokkum & Conroy (2010), but were such measurements made, Fig. 4 could be used to determine the accuracy needed in the measurements to allow for constraining the IMF. The effect of a bottom-heavy IMF on the CO_{KG} index is approximately (calculated in the same way as for the D_{CO} index) 11%. Also note that we could theoretically further tighten the spread in the CO indices by calibrating the metallicities of the SSP and exponentially declining SFR models, as discussed in Section 4.4. Finally, If we in Fig. 4 and Fig. 6 only look at the supposedly more realistic models with exponentially declining SFR, we can see that the effect of a bottom-heavy IMF is amplified by almost a factor of 2.

In theory, as there currently in fact exists D_{CO}, metallicity and age data for one of the interesting galaxies in van Dokkum, (NGC 4261) we could now proceed to run a new set of models centered around the metallicity of the interesting galaxy, and subsequently determine the IMF in the galaxy from the results. However, this is shown to be impossoble in Section 6.1. Regrettably the models in Table 1 do not immediately agree with observational data. In Section 7.1 we will investigate the possibility of correcting the calculations presented in this section.
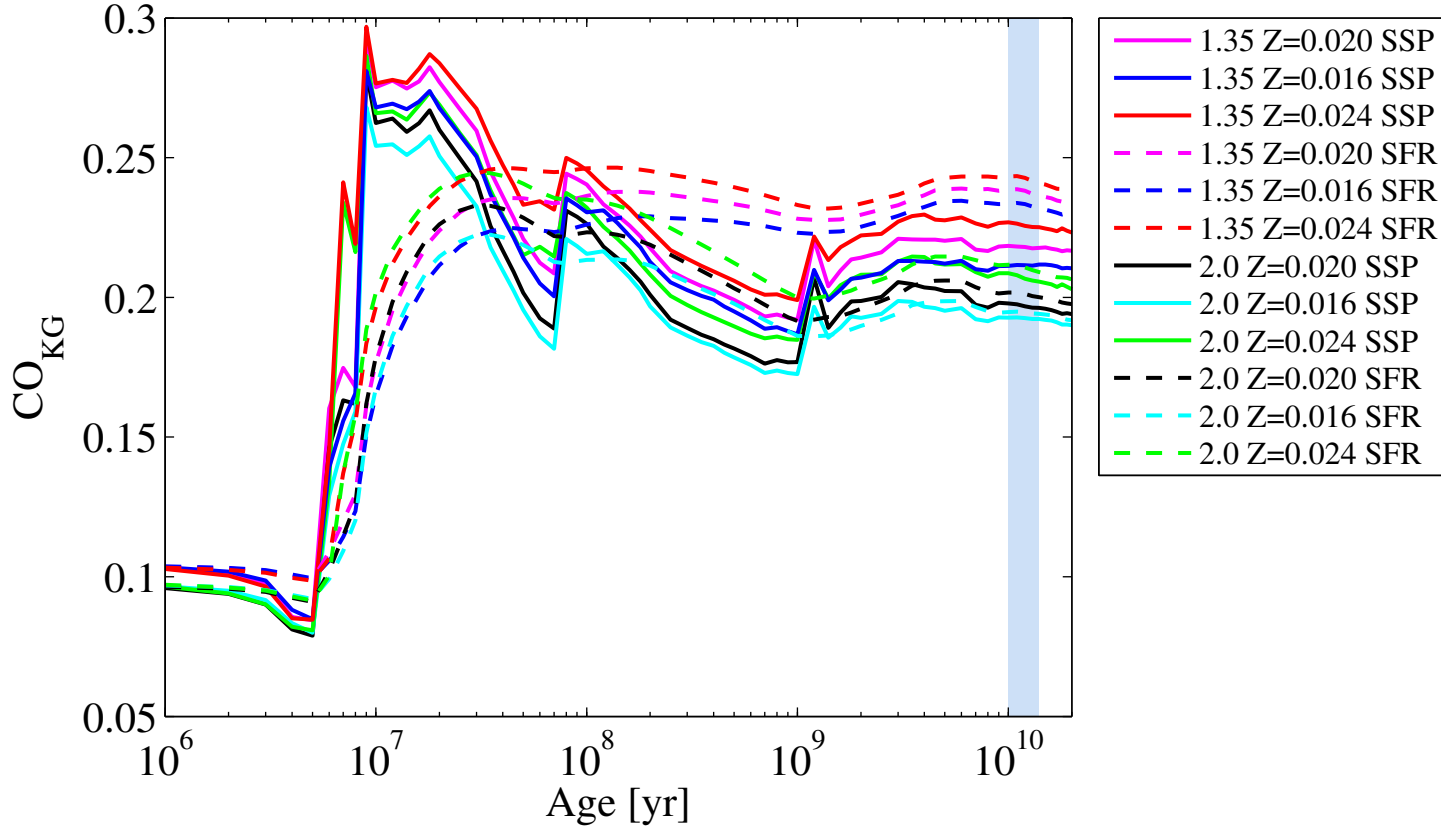
Fig. 3.— Synthetic calculations of the CO_{KG} index on spectra generated by PEGASE-HR. The colored interval represents age = 10-14 Gyr, which is where we reasonably can expect most giant ellipticals to be found (Yamada 2004). The legend should be interpreted as follows: The initial entry represents the slope of the IMF, i.e. the value for Γ in Eq. 1. The second entry represents the metallicity as the metallicity mass fraction Z. The last entry determines the star formation history, with SSP meaning an instantaneous burst, and SFR meaning an exponentially declining star formation rate. Models 1-13 in Table 1 have been used.
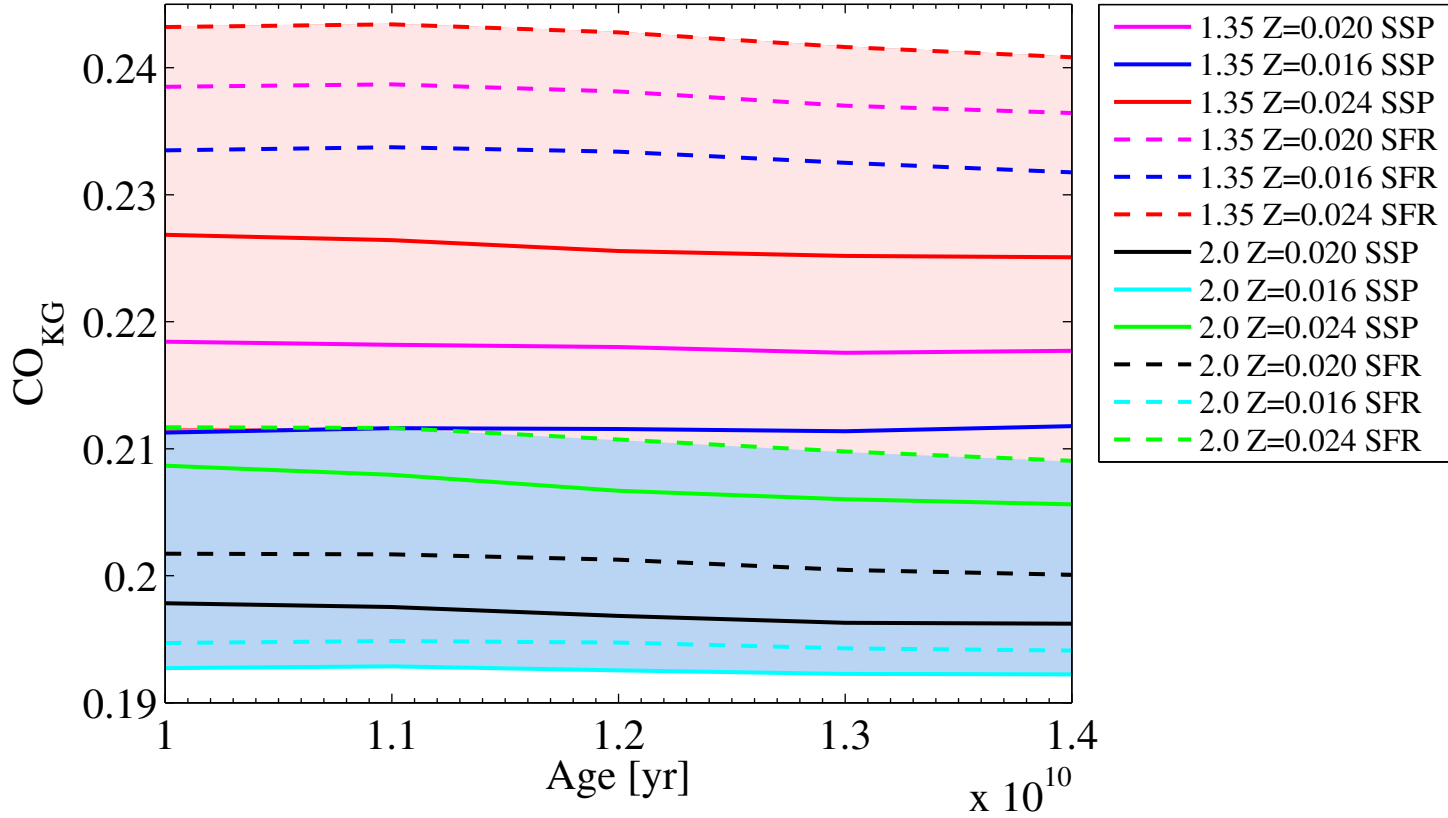
Fig. 4.— Synthetic calculations of the CO_{KG} index on spectra generated by PEGASE-HR at age = 10-14 Gyr. The area colored red represents the entire span of the models with a Salpeter IMF and the area colored blue represents the span of the models with a bottom-heavy IMF. The same models as in Fig. 3 have been used and the legend should be interpreted the same way as in Fig. 3.
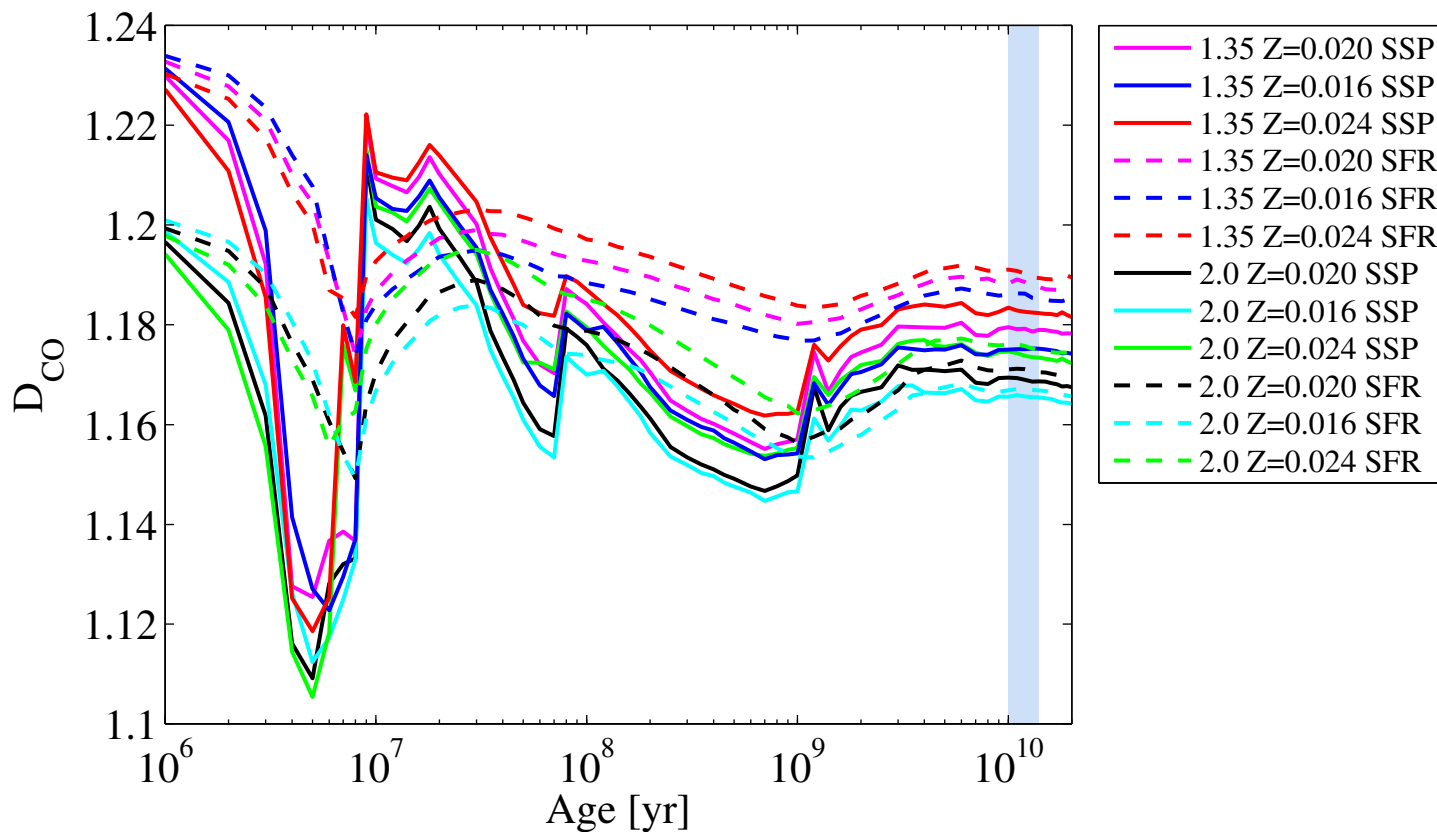
Fig. 5.— Synthetic calculations of the D_{CO} index on spectra generated by PEGASE-HR. The colored interval represents age = 10-14 Gyr, which is where we reasonably can expect most giant ellipticals to be found (Yamada 2004).The same models as in Fig. 3 have been used and the legend should be interpreted the same way as in Fig. 3.

Fig. 6.— Synthetic calculations of the D_{CO} index on spectra generated by PEGASE-HR at age = 10-14 Gyr. The area colored light red represents the entire span of the models with a Salpeter IMF and the area colored blue represents the span of the models with a bottom-heavy IMF. The area colored dark red represents the area where the D_{CO} values from the two IMFs overlap. The same models as in Fig. 3 have been used and the legend should be interpreted the same way as in Fig. 3.

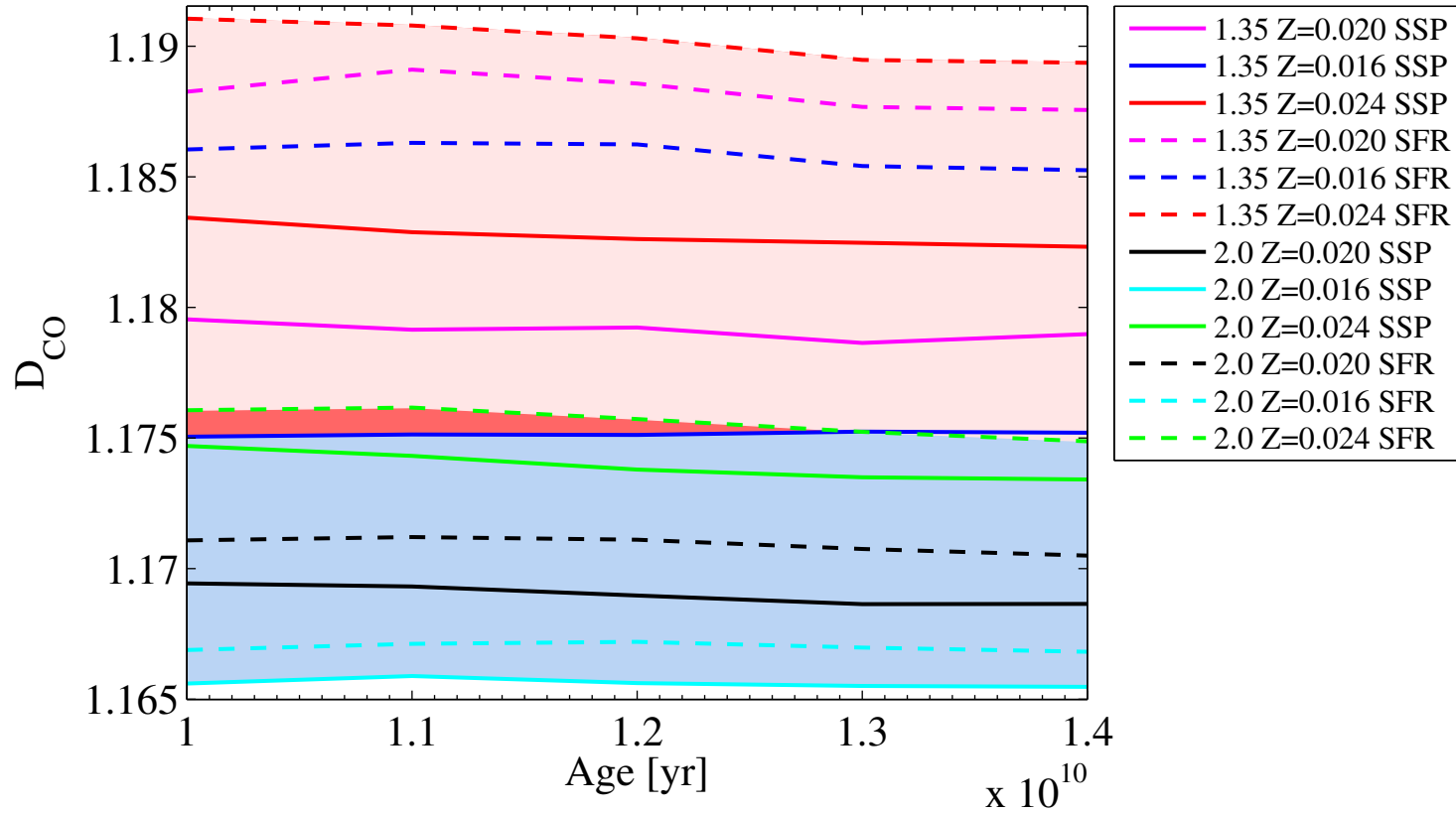### 6.1. Observational data for the CO_{KG} and D_{CO} indices

Observational and earlier synthetic data for a selection of elliptical galaxies can be found in K&G, which in addition to the synthetic CO_{KG} data calculated by K&G contains observational CO index measurements by Frogel et al. (1978). The synthetic CO_{KG} calculations by K&G are in good agreement with the values observed by Frogel et al. (1978). The CO data in Frogel et al. (1978) are measured directly with the help of physical filters and the CO_{KG} index in K&G is designed to match the filters used by Frogel et al. (1978). We have used the same CO index definition as K&G for the purpose of validating our model with the help of the available data, but when comparing the CO_{KG} values in Fig. 4 with the data from K&G, we can immediately see that even when looking at a much more generous time-interval, all the calculations on the synthetic spectra generated by PEGASE-HR result in CO_{KG} values that are very high in comparison (a typical value in K&G is CO_{KG}=0.140, for NGC 4478). When investigating the metallicities of the galaxies in K&G we can see that most of them in fact have a higher than solar metallicity, meaning that their CO_{KG} values would according to our models be expected to be higher than what we have calculated in Fig. 4, which is definitely not the case. The values for the CO_{KG} index obtained by K&G originate from spectral synthesis done on a stellar library consisting of observed stellar spectra. This is in contrast to the BaSeL library that has been used by PEGASE-HR. The BaSeL library is an entirely synthetic stellar atmosphere library where the spectra for all the stars have been theoretically calculated. The discrepancy realized above warrants an investigation of the theoretical spectra. This is done in Section 7. A comparison of the data in Figure 5 and 6 with observational D_{CO} data in Mármol-Queraltó et al. (2009) further confirms that there is a discrepancy between our models and observational data, even when accounting for the metallicity of the galaxies, however, this time our models result in D_{CO} values that are substantially lower than the observations, this might appear strange but it is in fact not unexpected as the index definitions are different; by looking at Fig. 3 and Fig. 5 we can immediately detect big differences in the behavior of the indexes especially in the earlier stages of the evoultion of the galaxies. However, from the analysis above it is clear that there is a problem with our models, and what immediately warrants closer inspection is the theoretical spectral library, BaSeL, used by PEGASE-HR as a basis for all the evolutionary synthesis.

7. Investigating the reliability of the BaSeL library

In panel a) of Fig. 7 we show D_{CO} calculations as a function of $4050/T_{eff}$ for the entire dataset from the recent stellar library developed by Mármol-Queraltó et al. (2008), along with D_{CO} calculations done on data from three different metallicites from the BaSeL library by Lejeune et al. (1997). A clear discrepancy across the entire spectrum of effective temperatures can immediately be seen. Also note that panel a) of Figure 7 can directly be compared with Fig. 13 in Mármol-Queraltó et al. (2008), confirming that there is not a problem with the D_{CO} calculations themselves. With the discovery of this discrepancy in mind, we are regrettably forced to be quite sceptical about all

the results obtained with the PEGASE-HR model. However, we can still see that on the whole the spectra in BaSeL appear to rougly follow the same behavior as a funtion of the effective temperature as the observed spectra by Mármol-Queraltó et al. (2008). This at least gives some indication that the calculations in the earlier sections are not vastly incorrect. In panel b) of Figure 7 we show the same datasets but with a fit-by-eye shift of -0.0018 applied to the BaSeL values. No real analysis has been made, but with this shift it could definitely be argued that we have achieved a better agreement between the datasets. We will investigate the effect of applying a shift to the data in Section 6 in Section 7.1. However, upon even closer inspection of the Lejeune and M??rmol-Queralt?? libraries, one can show that the discrepancy also has a temperature dependence. For low temperatures the D_{CO} index is too low in the BaSeL library and for high temperatures it is too high. This means that correcting by a simple shift in Section 6 will not be optimal. This is why we have chosen not to pursue this to any great extent, as it is likely that it would in fact be easier to use an entirely new spectral library instead of trying to calibrate the BaSeL library in some complicated fashion.

7.1.   Possible solutions

Here we will investigate the effect of applying a data-shift to the calculations in Section 6. However, to do this we will need D_{CO} data for as many galaxies as possible. We also have to restrict ourselves to galaxies of similar metallicity due to the large influence of the metallicity on the CO absorption. In Table 3 we show compiled age, metallicity and D_{CO} measurements, where available, for all galaxies with comparatively similar metallicity included in the entire study by Mármol-Queraltó et al. (2009). Two interesting manual shifts are presented in Figures 8 and 9. The shift in Fig. 9 represents the lowest possible shift we can apply with no galaxies exclusively in the bottom-heavy IMF D_{CO}-range. We can see that we have two clear outliers, NGC 1316 and NGC 4564. However, NGC 4564 also has the highest metallicity, [Fe/H]=0.44, and it can be argued that it should possibly have been left out entirely. Additionally, NGC 1316 is not a true elliptical galaxy and is possibly not modeled adequately by our spectral synthesis. So, in the most conservative scenario[1] if we remove the S0 galaxies and NGC 4564 from the data all of the galaxies are compatible with a Salpeter IMF. Fig. 8 shows an attempt at fitting all of the galaxies as close to the entire D_{CO}-span of the two IMFs as possible. No conclusions as to the quality of the fit in Fig. 8 can really be made with only this as the basis, but looking at Fig. 8 we can see that it is just barely possible to fit all the galaxies into the entire span of the D_{CO} data from the two IMFs. Note that this fit in fact seems quite reasonable; we know that using the full span of our models should result in a metallicity interval that is bigger than 0.2 dex with the metallicity evolution of the SFR models in mind. The full metallicity span of the galaxies in Fig. 8 is 0.27 dex, i.e. fairly similar to the model

---

[1]This scenario with the S0 galaxies removed to restrict us to pure elliptical galaxies and NGC 4564 removed to further limit the metallicity spread is arguably closest to the scenario modeled by our spectral synthesis.

assumptions. This result in itself would support the van Dokkum hyphothesis that the IMF is not universal. To fit all of these galaxies in the range of just one of the IMFs it would likely require a metallicity spread in PEGASE-HR much larger than the observed 0.27 dex interval; the interval needed to cover the entire CO spread in the galaxies in Table 3 is close to two times as large as the D_{CO} interval calculated with our models that already cover a larger than 0.2 dex interval centered around the solar metallicity, Z=0.02. However this has not been thoroughly tested so we cannot really make any statements. It is possible that all of the galaxies in Table 3 could be fitted to the Salpeter IMF with a more exact metallicity interval used in PEGASE-HR; even with the models displayed in Fig. 8 and Fig. 9 we can see that more galaxies can be fitted (by further shifting of the models) into the Salpeter IMF (7 at most) vs. the bottom-heavy IMF (5 at most). On the other hand, under the quite generous assumptions that the lenticular galaxies are also adequately modeled, and that there exists two populations of elliptical galaxies, one with a Salpeter IMF, and one population with a bottom-heavy IMF, Fig. 8 could definitely be considered the better fit, as we can practically fit all of the galaxies in the span of the modeled D_{CO} data. The shift in Fig. 8 puts NGC 4261 with a high probability in the bottom-heavy range, also supporting the van Dokkum & Conroy hypothesis. To conclusively address the the choice of the data-shift, more D_{CO} data would be needed, or we could possibly use some other method for calibrating the shift. One method could be to calibrate the D_{CO} index against globular clusters, where we know that the IMF is not bottom-heavy, shown for example in Schaerer & Charbonnel (2011). This has however not been attempted in this project. Ultimately one should at least note that if the calculations were vastly wrong in Section 6, it would be very unlikely that we could produce such suprisingly good data-fits in Fig. 8 and Fig. 9. Even though we cannot really reach any definite conclusions with these two shifts, Figures 7, 8 and 9 can at least be interpreted as support for the validity of the conclusions made in Section 6.
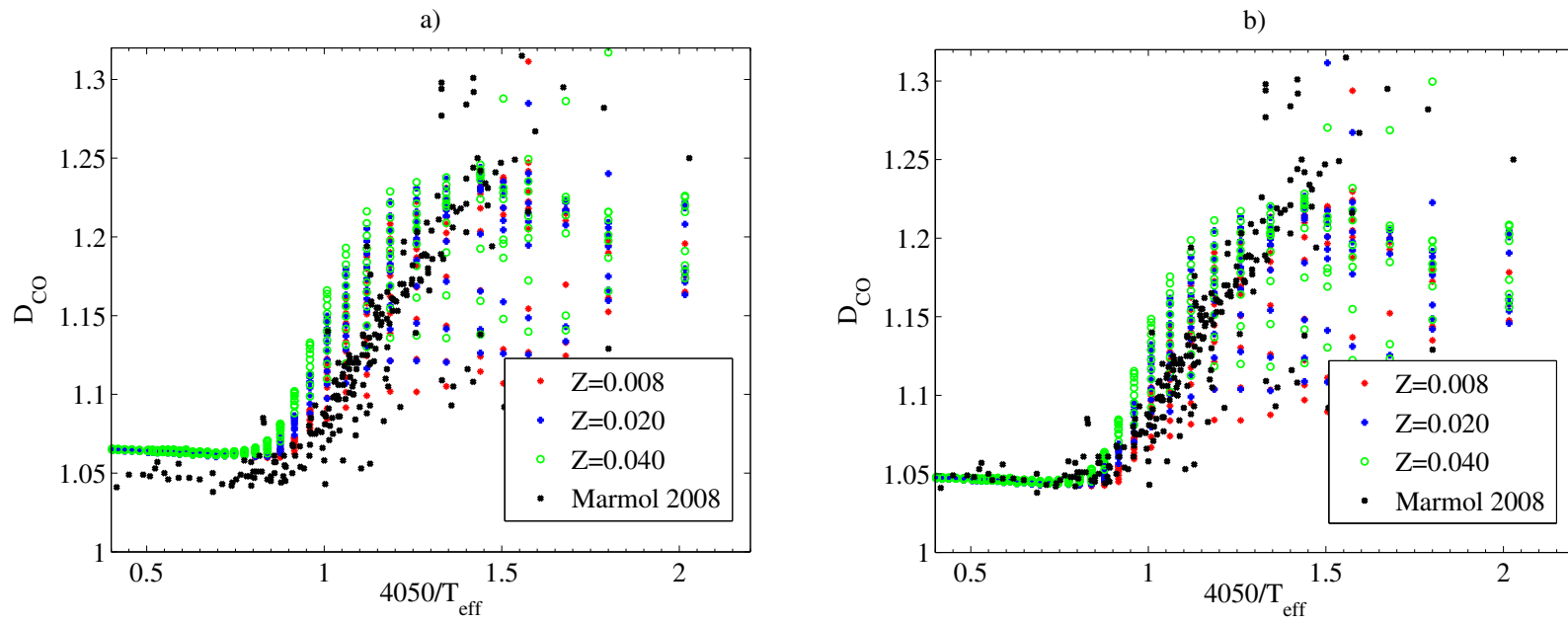
Fig. 7.— D_{CO} calculations for the BaSeL and Mármol-Queraltó et al. (2008) stellar libraries. In a) we show as the black dots D_{CO} calculations as a function of $4050/T_{eff}$ done on the entire dataset from the recent stellar library developed by Mármol-Queraltó et al. (2008). The RGB colored dots represent D_{CO} calculations for three different metallicites from the BaSeL library by Lejeune et al. (1997). In b) we show the same calculations but with a fit-by-eye shift of -0.0018 applied to the BaSeL D_{CO} values.

Fig. 8.— Synthetic calculations of the D_{CO} index on spectra generated by PEGASE-HR at age = 1-15 Gyr. All values shifted by +0.03725. The area colored light red represents the entire span of the models with a Salpeter IMF and the area colored blue represents the span of the models with a bottom-heavy IMF. The area colored dark red represents the area where the D_{CO} values from the two IMFs overlap. Note that with this shift we can just ba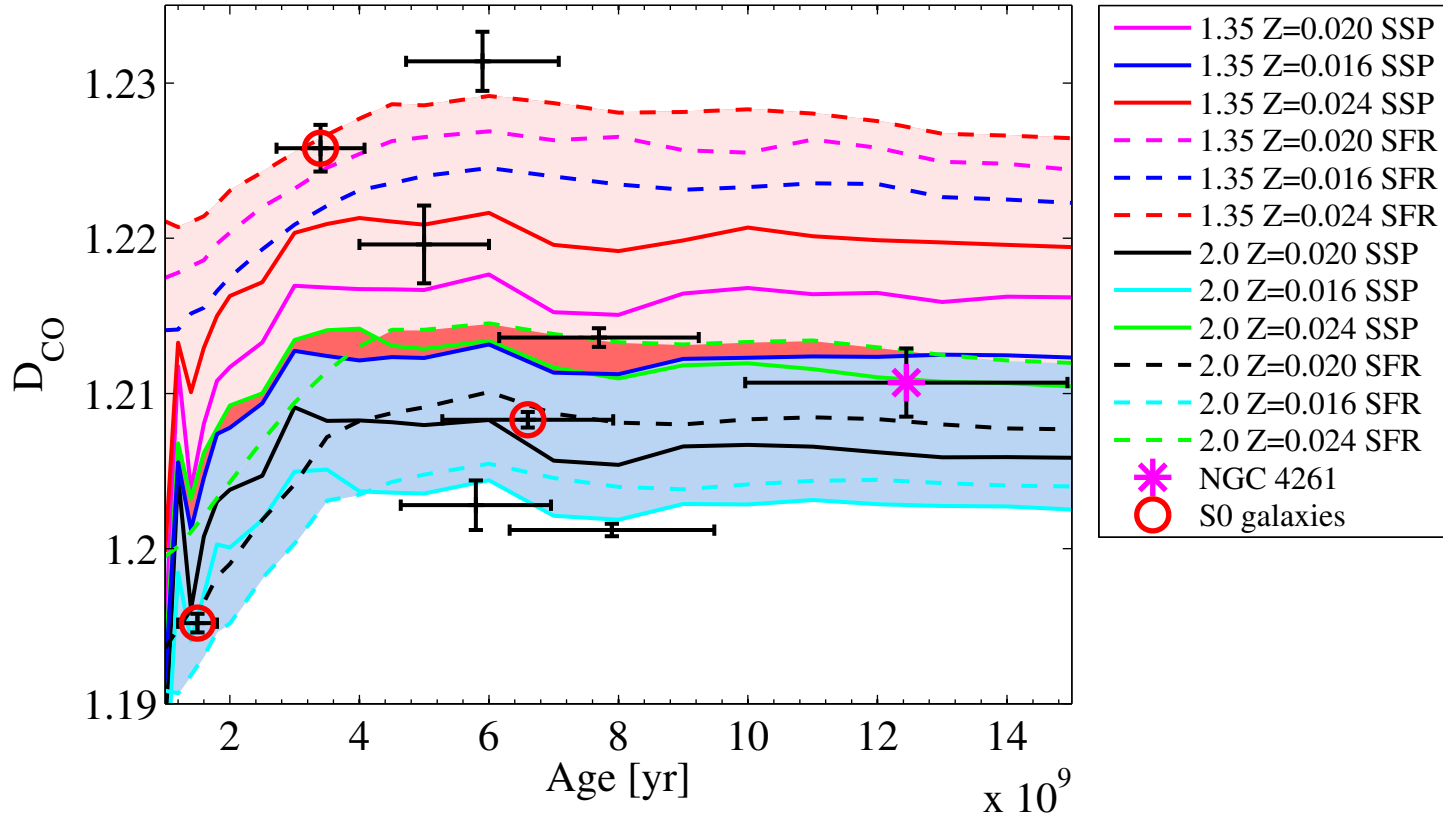rely include all of the galaxies in the span of the two IMFs, and this would put the van Dokkum galaxy NGC 4261 in the bottom-heavy IMF range with a high probability. The legend should be interpreted as follows: The initial entry represents the slope of the IMF, i.e. the value for Γ in Eq. 1. The second entry represents the metallicity as the heavy mass fraction. The last entry determines the star formation history, with SSP meaning an instantaneous burst, and SFR meaning an exponentially declining star formation rate. The black dots with errorbars represent the data in Table 3. Models 1-13 have been used. Check Table 1 for a complete list of the parameters used while running PEGASE-HR.
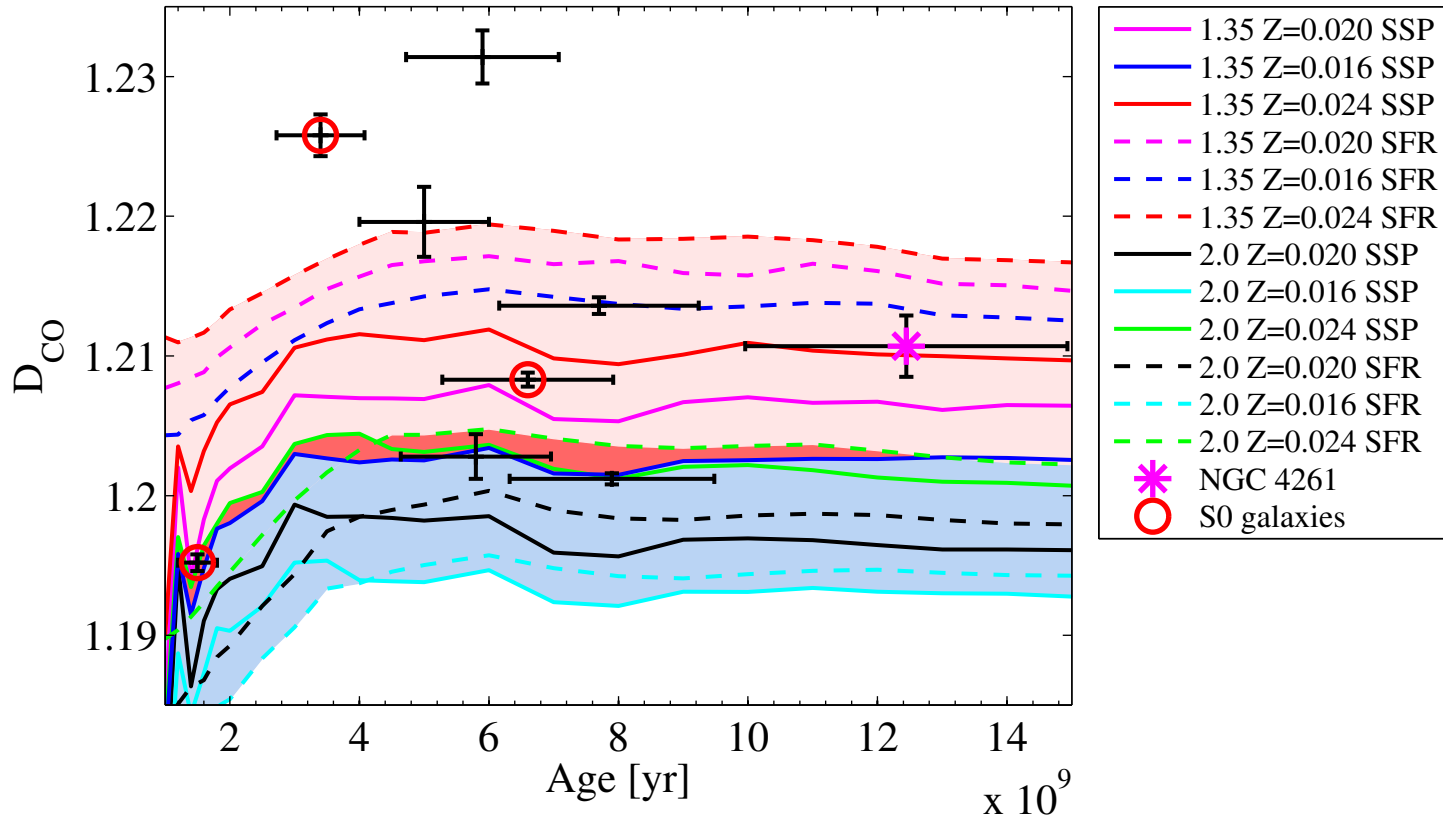
Fig. 9.— Synthetic calculations of the D_{CO} index on spectra generated by PEGASE-HR at age = 1-15 Gyr. All values shifted by +0.0275. The area colored light red represents the entire span of the models with a Salpeter IMF and the area colored blue represents the span of the models with a bottom-heavy IMF. The area colored dark red represents the area where the D_{CO} values from the two IMFs overlap. The same models as in Fig. 8 have been used and the legend should be interpreted the same way as in Fig. 8. Note that except for the two uppermost galaxies that possibly should be excluded from the data (see Section 7.1) the galaxies, including NGC 4261, are all compatible with a Salpeter IMF.

8. Additional data generated by PEGASE-HR

The main focus of this project is CO absorption and the CO index at around 2.3 μm, but because it is easily made available with PEGASE-HR and our already constructed models, we will in this section present and briefly investigate the effect of a bottom-heavy IMF on the M/L_V ratio and the V-I_C color index.

8.1. The M/L_V ratio

In Fig. 10 the stellar[1] M/L ratio has been calculated using synthetic luminosity and mass data generated by PEGASE-HR. Panel a) in Fig. 10 shows the M/L_V ratio as a function of galaxy age for a Salpeter, a bottom-heavy IMF with Γ = 2.0, and a Kroupa IMF (Kroupa 2002). We can clearly see that a bottom-heavy IMF predicts the highest stellar M/L_V ratios. In panel b) of Fig. 10 we show that observational *effective radius*[2] mass-to-light ratio measurements by van der Marel & van Dokkum (2007) on the van Dokkum galaxies in Table 2 are in good agreement with synthetic PEGASE-HR stellar M/L data. On first glance the data in van der Marel & van Dokkum (2007) is best fitted to a Salpeter IMF or something slightly more bottom-heavy, however in any observational M/L mesurements it is hard to determine the M/L ratio for only the stellar content, as there, regardless of the radius used to dynamically calculate the mass, will always at least be some dark matter included in the mass measurement, shifting the data towards higher M/L values compared to the true stellar M/L ratios. It is hard to say if the effect of dark matter in the data by van der Marel & van Dokkum (2007) is large enough to change what IMF achieves the best fit in panel b) of Fig. 10 without a thorough investigation. However, note that accounting for the DM can only result in lower observed M/L ratios, making them even less consistent with the bottom-heavy IMF scenario proposed by van Dokkum & Conroy (2010). This finding is confirmed in van Dokkum & Conroy (2010) where it is briefly noted that their best-fitting IMF (bottom-heavy Γ = 2.0) does in fact not appear to be consistent with the observed M/L evolution of massive cluster galaxies (see also Section 8.3 for a discussion about the observed M/L ratios). For mass-to-light ratio calculations using larger radii than the effective radius the M/L ratio increases dramatically as a function of the radius included in the dynamical mass calculation (Buote & Humphrey 2011), thus, with the confirmation of the need for dark matter in elliptical galaxies (Buote & Humphrey 2011), the currently most popular approach is to explain high observational mass-to-light ratios, e.g. (King & Minkowski 1972; Schechter 1980; Bacon et al. 1985), by assuming a "normal" IMF (Salpeter or Kroupa IMF) and by assuming that the high values are caused by the dark matter

---

[1]The stellar mass includes the mass in stars, white dwarfs, neutron stars and black holes.

[2]The mass-to-light ratio data in van der Marel & van Dokkum (2007) is calculated within an effective radius where the M/L ratio is practically constant (Kronawitter et al. 2000), minimizing the influence of the dark matter content.

content. In Buote & Humphrey (2011) it is indeed shown that the best stellar M/L ratio fits are obtained with a Kroupa IMF when minimizing the influence of dark matter using DM profiles to eliminate the dark matter contribution to the dynamical mass calculations for the measured galaxies. Spiniello et al. (2011) also use lensing and dynamics constraints to rule out (> 90% C.L) a bottom-heavy IMF with $\Gamma = 2.0$ in the early-type galaxy SDSS J1148+1930.

8.2. The V-I_C color index

In Fig. 11 we present the V-I_C[1] color index as a function of galaxy age. Fig. 11 includes models for both a bottom-heavy IMF and a regular Salpeter IMF. In panel b) of Fig. 11 we also show V-I_C data by Buta & Williams (1995), which appears to be relatively compatible with a Salpeter IMF. However, about half of the galaxies lie completely out of the range of the models, so it appears that there might be an age calibration problem (see also Section 8.3). Subsequently, we cannot really use Fig. 11 to say anything about the IMF, but it does confirm that PEGASE-HR generates V-I_C color index data that lies in the correct ballpark compared to observations. However, we can in any case see that a bottom-heavy IMF does in fact have an effect on the V-I_C color index. At age = 10 Gyr models with a bottom-heavy IMF predicts approximately 4.7% higher V-I_C color index values (calculated at the center of the areas covered by the two IMFs). Typically the size of the error intervals in the V-I_C data in Buta & Williams (1995) are on the order of 1.4% of the measured V-I_C values. The effect of a bottom-heavy IMF is larger than the typical error intervals, in the best cases by about a factor of 4, so it might be possible to pursue this further, however, in Section 6.1, Fig. 8 and Fig. 9 we have shown that this error-effect ratio is better for the D_{CO} index. The errors in Buta & Williams (1995) might also have to be seen as optimistic. In the more recent paper by Idiart et al. (2003) more emphasis is put on calculating the total error for the V-I color index, and this results in larger total errors percentage-wise: around 3% for NGC 4261. In conclusion, we consider the CO index to be a better candidate method than the V-I_C color index for investigating the IMF in giant ellipticals.

8.3. Discussion

In Sections 8.1 and 8.2 we have shown that synthetic PEGASE-HR V-I_C color index and stellar M/L ratio calculations appear to be incompatible with a bottom-heavy IMF scenario with $\Gamma = 2.0$. However, a solution to this problem can possibly be found in the SFH of the galaxies. As discussed in Section 2 it is likely that Eq. 2 is in fact unrealistic. If giant elliptical galaxies formed in large mergers followed by sporadic smaller mergers (Kaviraj et al. 2009) during the entire life of the

---

[1]We are using the VRI system by Cousins (1976). The V-I_C color index compares the flux in the V (visual) band and the I_C band defined by Cousins (1976). See also Bessell (1979) and Bessell (2005) for a review of the Cousins VRI system and other standard photometric systems.

galaxies, it is possible that a more realistic description of the SFR would be an SFR with the same general shape as Eq. 2 but with the addition of a possibly large number of randomly distributed smaller spikes (caused by the smaller mergers) that are very short in duration. We have shown in Fig. 11 that the V-I_C color index increases as a function of the age of the stellar population in the modeled elliptical galaxies, thus the presence of younger stellar poulations would in theory result in a lower observed V-I_C color index. Similarly (see Fig. 10), the observed stellar M/L ratio will also be lower if the galaxy contains younger stellar populations. As we can see, it is in theory possible that non-standard star formation histories could allow the van Dokkum glaxies studied in this paper to have low observed M/L and V-I_C ratios while still in reality having bottom-heavy IMFs. However, we know that most giant ellipticals should be dominated by old stellar populations, so the presence of bursty SFHs would in practice have to be investigated separately in all of the van Dokkum galaxies. If evidence of recent bursts are found, the effect on the observed V-I_C and M/L data would then in turn have to be thoroughly investigated in order to reach any possible conclusions about the compatibility to a bottom-heavy IMF.
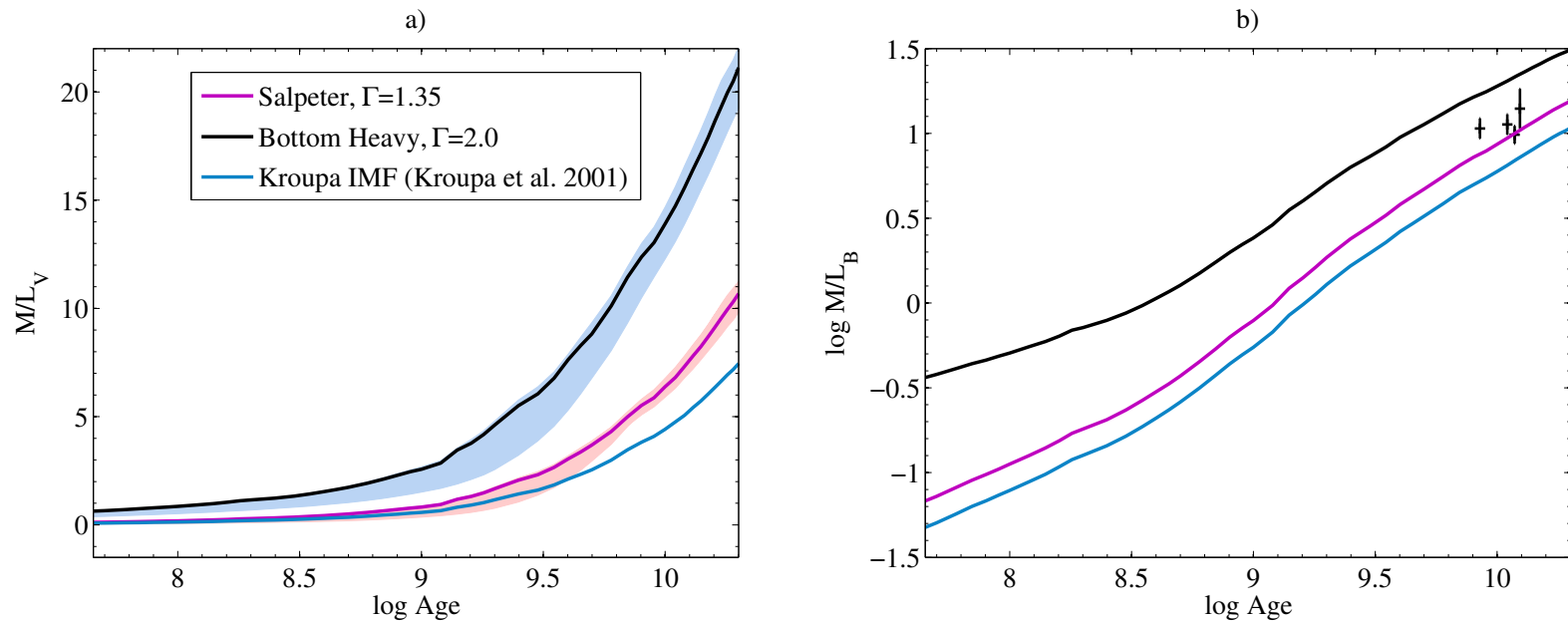
Fig. 10.— Synthetic calculations of mass-to-light ratios on data generated by PEGASE-HR as a function of galaxy age. The colored lines represent the different IMFs for SSPs with solar metallicity. Panel a) shows the stellar M/L_V ratio in units of $M_\odot/L_{V_\odot}$. The colored areas in panel a) illustrate the uncertainty induced by the metallicity and SFR range of the models discussed in Section 4. Panel b) shows log (M/L_B) in units of log $(M_\odot/L_{B_\odot})$. The black errorbars in panel b) represent the M/L_B data in Table 2. We can see that synthetic M/L_B data from PEGASE-HR is in good agreement with observational M/L_B measurements (van der Marel & van Dokkum 2007). Models 1-14 have been used. Check Table 1 for a complete list of the parameters used in the models while running PEGASE-HR.
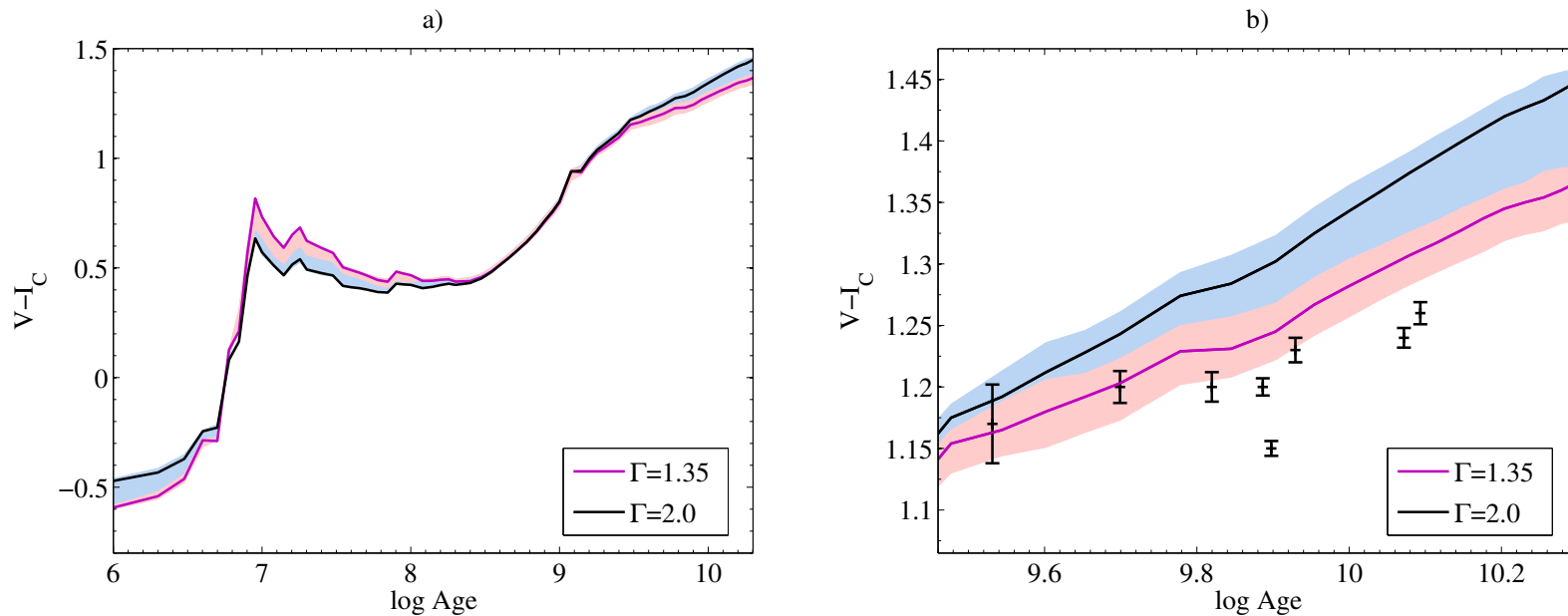
Fig. 11.— The V-I_C color index data as a function of galaxy age generated by PEGASE-HR. In a) we show the V-I_C color index for the entire life of a galaxy. In b) we show the V-I_C color index for age = 3 - 20 Gyr. The area colored light red represents the entire span of the models with a Salpeter IMF and the area colored blue represents the span of the models with a bottom-heavy IMF. The errorbars represent V-I_C data from Buta & Williams (1995), where available, for the galaxies in Table 1 and Table 2. Models 1-13 in Table 1 have been used.

9. Conclusions

The ultimate goal of this project is to theoretically determine if the change in CO absorption due to a bottom heavy IMF with $\Gamma = 2.0$ is large enough to overcome current observational uncertainties in the age and the metallicity along with possible variations in the SFR for giant elliptical galaxies. Although there appears to be some problems with the BaSeL library, it is still considered very likely that it is possible to constrain the IMF in giant ellipticals by analyzing the CO absorption, preferrably using the D_{CO} index (Fig. 6). We are reluctant to make any definite claims due to the findings that the BaSeL library is not entirely accurate in the CO-region (Section 7). However, Fig. 7, 8 and 9 result in the hypothesis that the big problem is in the absolute values of the index calculations, not in the general behavior of the absorption band when the slope of the IMF changes from Salpeter to bottom-heavy. However, we have not investigated the accuracy of the BaSeL library in detail for all stellar masses, so we have to bear in mind that if the library is very inaccurate in the CO region for the low mass stars, the effect of a bottom-heavy IMF will of course be overestimated. It is likely that the simplest approach would be to construct a new SSP model using empirical spectra in the CO region.

In Fig. 8 we can see that by shifting the D_{CO} index values we can arrive at a suprisingly interesting, although only speculative, result that can be interpreted as support for a bottom heavy IMF in one of the galaxies (NGC 4261) studied by van Dokkum & Conroy (2010). However, in Spiniello et al. (2011) a bottom-heavy IMF is ruled out in the early-type galaxy SDSS J1148+1930. And in Buote & Humphrey (2011) it is shown that after accounting for dark matter the observational M/L ratio in many of the galaxies studied by van Dokkum & Conroy (2010) are compatible with SSP models with a Kroupa IMF. In Section 8.1 we independently show that a very bottom-heavy IMF in PEGASE-HR, such as the IMF propsed by van Dokkum & Conroy (2010) with $\Gamma = 2.0$, appears to be incompatible with M/L ratio observations by van der Marel & van Dokkum (2007) for some of the van Dokkum galaxies in Table 2. On the other hand, in addition to the results by van Dokkum & Conroy (2010) more evidence for a non-universal IMF is presented in van Dokkum & Conroy (2011). Additionally, it is possible that the observed M/L ratio and V-I_C color index data that has been shown to be incompatible with a bottom-heavy IMF could be explained by the presence of younger stellar populations in the observed galaxies. The IMF debate is definitely not settled, so it still seems worth the effort to continue to investigate the CO index as a tool for determining the IMF in giant ellipticals. What needs to be done would ideally be to use a modern stellar library in the CO region, such as Mármol-Queraltó et al. (2008), in the stellar population synthesis. There currently exists D_{CO}, metallicity and age data for one of the galaxies that are shown to fit best to a bottom-heavy IMF in van Dokkum & Conroy (2010), so a new SPS model using correct spectra in the CO region could most likely immediately be used to check van-Dokkums results. Even if the use of a better stellar library is shown to exhibit a smaller influence on the CO region due to a bottom-heavy IMF, it might still be possible to use more accurate future metallicity measurements to constrain the IMF, and even with no improvement in metallicity measurements, it might still be possible to further improve the method used in this project by more closely investigating the SFH for elliptical galaxies. We showed in Fig. 4 and Fig. 6, that the ef-

fect of a bottom-heavy IMF is enhanced in PEGASE-HR assuming an exponentially declining star formation. For future work in constraining the IMF in giant ellipticals we would rank in order of importance: the use of a stellar library with empirical spectra in the CO region, the use of a more accurate SFR for elliptical galaxies and finally the use of more recent and improved metallicity measurements.

REFERENCES

Annibali, F., Bressan, A., Rampazzo, R., Zeilinger, W. W., & Danese, L. 2007, A&A, 463, 455

Asplund, M., Grevesse, N., Sauval, A. J., Allende Prieto, C., & Kiselman, D. 2004, A&A, 417, 751

Bacon, R., Monnet, G., & Simien, F. 1985, A&A, 152, 315

Bernardi, M., Shankar, F., Hyde, J. B., et al. 2010, MNRAS, 404, 2087

Bessell, M. S. 1979, PASP, 91, 589

Bessell, M. S. 2005, ARA&A, 43, 293

Bolton, A. S., Treu, T., Koopmans, L. V. E., et al. 2008, ApJ, 684, 248

Buote, D. A. & Humphrey, P. J. 2011, ArXiv e-prints, 1104.0012

Buta, R. & Williams, K. L. 1995, AJ, 109, 543

Cousins, A. W. J. 1976, MmRAS, 81, 25

De Lucia, G., Springel, V., White, S. D. M., Croton, D., & Kauffmann, G. 2006, MNRAS, 366, 499

Fioc, M. & Rocca-Volmerange, B. 1997, A&A, 326, 950

Fioc, M. & Rocca-Volmerange, B. 1999, ArXiv Astrophysics e-prints, 9912179

Frogel, J. A., Persson, S. E., Matthews, K., & Aaronson, M. 1978, ApJ, 220, 75

Frogel, J. A., Stephens, A., Ramírez, S., & DePoy, D. L. 2001, AJ, 122, 1896

Grebel, E. K. 2011, in IAU Symposium, Vol. 270, IAU Symposium, ed. J. Alves, B. G. Elmegreen, J. M. Girart, & V. Trimble, 335–346

Iben, Jr., I. 1991, ApJS, 76, 55

Idiart, T. P., Michard, R., & de Freitas Pacheco, J. A. 2003, A&A, 398, 949

Jeffery, C. S. 2010, in Principles and Perspectives in Cosmochemistry, ed. A. Goswami & B. E. Reddy, 3–642

Kaviraj, S., Peirani, S., Khochfar, S., Silk, J., & Kay, S. 2009, MNRAS, 394, 1713

Kennicutt, Jr., R. C. 1998, ARA&A, 36, 189

King, I. R. & Minkowski, R. 1972, in IAU Symposium, Vol. 44, External Galaxies and Quasi-Stellar Objects, ed. D. S. Evans, D. Wills, & B. J. Wills, 87–+

Knapp, G. R. 1999, in Astronomical Society of the Pacific Conference Series, Vol. 163, Star Formation in Early Type Galaxies, ed. P. Carral & J. Cepa, 119–+

Kormendy, J., Fisher, D. B., Cornell, M. E., & Bender, R. 2009, ApJS, 182, 216

Kotulla, R., Fritze, U., Weilbacher, P., & Anders, P. 2009, MNRAS, 396, 462

Kronawitter, A., Saglia, R. P., Gerhard, O., & Bender, R. 2000, A&AS, 144, 53

Kroupa, P. 2002, in Astronomical Society of the Pacific Conference Series, Vol. 285, Modes of Star Formation and the Origin of Field Populations, ed. E. K. Grebel & W. Brandner, 86–+

Kroupa, P. & Gilmore, G. F. 1994, MNRAS, 269, 655

Kroupa, P., Tout, C. A., & Gilmore, G. 1993, MNRAS, 262, 545

Le Borgne, D., Rocca-Volmerange, B., Prugniel, P., et al. 2004, A&A, 425, 881

Lejeune, T., Cuisinier, F., & Buser, R. 1997, A&AS, 125, 229

Lejeune, T., Cuisinier, F., & Buser, R. 1998, A&AS, 130, 65

Mármol-Queraltó, E., Cardiel, N., Cenarro, A. J., et al. 2008, A&A, 489, 885

Mármol-Queraltó, E., Cardiel, N., Sánchez-Blázquez, P., et al. 2009, ApJ, 705, L199

McDermid, R., Alatalo, K., Blitz, L., et al. 2011, in Bulletin of the American Astronomical Society, Vol. 43, American Astronomical Society Meeting Abstracts #217

McKee, C. F. & Ostriker, E. C. 2007, Ann.Rev.Astron.Astrophys., 45, 565

Mieske, S. & Kroupa, P. 2008, ApJ, 677, 276

Miller, G. E. & Scalo, J. M. 1979, ApJS, 41, 513

Naab, T. & Burkert, A. 2001, in Astronomical Society of the Pacific Conference Series, Vol. 230, Galaxy Disks and Disk Galaxies, ed. J. G. Funes & E. M. Corsini, 453–454

Raichoor, A., Mei, S., Nakata, F., et al. 2011, ApJ, 732, 12

Rogers, B., Ferreras, I., Peletier, R., & Silk, J. 2010, MNRAS, 402, 447

Salpeter, E. E. 1955, ApJ, 121, 161

Sánchez-Blázquez, P., Gorgas, J., Cardiel, N., & González, J. J. 2006, A&A, 457, 809

Sandage, A. 1986, A&A, 161, 89

Schaerer, D. & Charbonnel, C. 2011, MNRAS, 413, 2297

Schechter, P. L. 1980, AJ, 85, 801

Spiniello, C., Koopmans, L. V. E., Trager, S. C., Czoske, O., & Treu, T. 2011, ArXiv e-prints, 1103.4773

Terlevich, A. I. & Forbes, D. A. 2002, MNRAS, 330, 547

van der Marel, R. P. & van Dokkum, P. G. 2007, ApJ, 668, 756

van Dokkum, P. & Conroy, C. 2011, ArXiv e-prints, 1102.3431

van Dokkum, P. G. & Conroy, C. 2010, Nature, 468, 940

Vazdekis, A., Sánchez-Blázquez, P., Falcón-Barroso, J., et al. 2010, in IAU Symposium, Vol. 262, IAU Symposium, ed. G. Bruzual & S. Charlot, 65–68

Yamada, Y. 2004, in Studies of Galaxies in the Young Universe with New Generation Telescope, ed. N. Arimoto & W. J. Duschl, 55–55

Table 1.   PEGASE-HR model parameters

Model	Type	IMF slope (Γ)	Z	$SFR\ p_1\ [Myr]$	$SFR\ p_2\ [M_\odot]$
1	SSP	1.35	0.020	$\cdots$	$\cdots$
2	SSP	1.35	0.016	$\cdots$	$\cdots$
3	SSP	1.35	0.024	$\cdots$	$\cdots$
4	SFR	1.35	0.020	1000	1
5	SFR	1.35	0.016	1000	1
6	SFR	1.35	0.024	1000	1
7	SSP	2.0	0.020	$\cdots$	$\cdots$
8	SSP	2.0	0.016	$\cdots$	$\cdots$
9	SSP	2.0	0.024	$\cdots$	$\cdots$
10	SFR	2.0	0.020	1000	1
11	SFR	2.0	0.016	1000	1
12	SFR	2.0	0.024	1000	1
13	SSP	Kroupa 2001	0.020	$\cdots$	$\cdots$
14	SSP	1.70	0.020	$\cdots$	$\cdots$
15	SSP	2.5	0.020	$\cdots$	$\cdots$
16	SSP	3.5	0.020	$\cdots$	$\cdots$
17	SSP	4.0	0.020	$\cdots$	$\cdots$
18	SSP	5.0	0.020	$\cdots$	$\cdots$

Note. — All parameters not contained in Table 1 has been left at the default values in PEGASE-HR.

Table 2.   Data for the galaxies studied by van Dokkum & Conroy (2010)

Galaxy	age [Gyr]	age ref	[Fe/H][a]	D_{CO}[b]	V-I$_{C}$[c]	log M/L$_{B}$[d]
NGC 4261	12.4	4	0.19	1.2107 ± 0.0022	1.26 ± 0.009	1.146 ± 0.116
NGC 4374	11.8 / 9.8 ± 3.4	2 / 1	0.12	$\cdots$	1.24 ± 0.008	0.992 ± 0.052
NGC 4472	8.5	2	0.24	$\cdots$	1.23 ± 0.010	1.029 ± 0.059
NGC 4649	11	2	0.30	$\cdots$	$\cdots$	1.053 ± 0.060
NGC 4840	6.6	2	0.32	$\cdots$	$\cdots$	$\cdots$
NGC 4926	13	2	0.08	$\cdots$	$\cdots$	$\cdots$
IC 3976	$\cdots$	$\cdots$	$\cdots$	$\cdots$	$\cdots$	$\cdots$
NGC 4889	9.7	4	$\cdots$	$\cdots$	$\cdots$	$\cdots$

[a]The source for [Fe/H] metallicity determinations is ref. 2

[b]The source for D$_{CO}$ is ref. 3

[c]The source for V-I$_{C}$ is ref. 5

[d]The source for log M/L$_{B}$ data is ref. 6

Note. — For the data from ref. 2 ages have errors $< \pm20\%$ and metallicity errors are $< \pm0.1$ dex.

References. — (1) Annibali et al. (2007); (2) Terlevich & Forbes (2002); (3) Mármol-Queraltó et al. (2009); (4) spectral synthesis by Sánchez-Blázquez et al. (2006); (5) Buta & Williams (1995); (6) van der Marel & van Dokkum (2007)

Table 3.   Data for a selection of the galaxies studied by Mármol-Queraltó et al. (2009)

Galaxy	Type	age [Gyr]	age ref	[Fe/H][a]	D_{CO}[b]	V-I$_C$[c]
NGC 3605	E4-5	5.8	1	0.22	1.2028 ± 0.0016	$\cdots$
NGC 3818	E5	5.0	1	0.39	1.2196 ± 0.0025	1.20 ± 0.013
NGC 4261	E2-3	12.4	2	0.19	1.2107 ± 0.0022	1.26 ± 0.009
NGC 4564	E6	5.9	1	0.44	1.2314 ± 0.0019	$\cdots$
NGC 1316	S0pec	3.4	1	0.25	1.2258 ± 0.0015	1.17 ± 0.032
NGC 1374	E0	7.7	1	0.32	1.2136 ± 0.0006	1.20 ± 0.007
NGC 1375	S0	1.5	1	0.24	1.1952 ± 0.0006	1.07 ± 0.014
NGC 1381	S0	6.6	1	0.23	1.2083 ± 0.0005	1.20 ± 0.012
NGC 1427	E4	7.9	1	0.17	1.2012 ± 0.0004	1.15 ± 0.006

[a]The source for [Fe/H] metallicity determinations is ref. 2

[b]The source for D_{CO} is ref. 3

[c]The source for V-I$_C$ is ref. 4

Note. — For the data from ref. 2 ages have errors < ±20% and metallicity errors are < ±0.1 dex.

References. — (1) Terlevich & Forbes (2002); (2) spectral synthesis by Sánchez-Blázquez et al. (2006); (3) Mármol-Queraltó et al. (2009); (4) Buta & Williams (1995)

A. Matlab code

A.1. D_{CO} index

```matlab
%DCO INDEX

%clear
close all
clear all

% parameters
age_plot=2e10; % yr

%import pegase spectra

%filename
file_peg1='SSPs/salp13.dat';
file_peg2='SSPs/salp20.dat';
file_peg3='SSPs/s20z08.dat';
file_peg4='SSPs/s20z12.dat';
file_peg5='SSPs/s13z08.dat';
file_peg6='SSPs/s13z12.dat';
file_peg7='SSPs/salp17.dat';
file_peg8='SSPs/s13r10.dat';
file_peg9='SSPs/s13r08.dat';
file_peg10='SSPs/s13r12.dat';
file_peg11='SSPs/s20r10.dat';
file_peg12='SSPs/s20r08.dat';
file_peg13='SSPs/s20r12.dat';

file_peg=[file_peg1 file_peg2 file_peg3 file_peg4 file_peg5 file_peg6 file_peg7 file_peg8 ...
    file_peg9 file_peg10 file_peg11 file_peg12 file_peg13];
k=13;%number of spectra

flux=zeros(1221,k); %initiate flux-matrix
%co_flux=zeros(1221,k.*68);
```

```matlab
r=1;
while (r≤k) ;%repeat procedure for all spectra

%skip past file header
%---
fid1=fopen(file_peg(1+15*(r-1):15+15*(r-1)));
slask='';
while (strcmp(slask,'********************************************************')≠1)
    slask=fscanf(fid1,'%s',1);
end
%
%---

slask2=fscanf(fid1,'%s',3); %skip 3 first entries, not interesting
wave=fscanf(fid1,'%e',1221); %read wavelengths
slask3=fscanf(fid1,'%s',61); %skip section

% gather spectra for all ages
%-----
i=1;
age=0;
while (age≠age_plot)
    age=fscanf(fid1,'%i',1).*1e6; % yr
    slask4=fscanf(fid1,'%s',18);
    fluxx=fscanf(fid1,'%e',1221);
    slask5=fscanf(fid1,'%s',61);
    flux(:,i)=fluxx;
    i=i+1;
end
%-----
%age procedure done

%fill flux vector from all files
evalc(['co_flux_' num2str(r) '=' mat2str(flux) ]);
fclose(fid1); %close files
r=r+1;
end

%%%%%%%%% CO index calculations
```

```matlab
%CO_0=0.564;
wave_interp=[21450:1:24050]'; %wave-points to use for interpolating the flux vector

for co=1:68;

%interpolation procdedure
co_flux_interp_1(:,co)=interp1(wave(857:883),co_flux_1(857:883,co),wave_interp,'linear');
co_flux_interp_2(:,co)=interp1(wave(857:883),co_flux_2(857:883,co),wave_interp,'linear');
co_flux_interp_3(:,co)=interp1(wave(857:883),co_flux_3(857:883,co),wave_interp,'linear');
co_flux_interp_4(:,co)=interp1(wave(857:883),co_flux_4(857:883,co),wave_interp,'linear');
co_flux_interp_5(:,co)=interp1(wave(857:883),co_flux_5(857:883,co),wave_interp,'linear');
co_flux_interp_6(:,co)=interp1(wave(857:883),co_flux_6(857:883,co),wave_interp,'linear');
co_flux_interp_7(:,co)=interp1(wave(857:883),co_flux_7(857:883,co),wave_interp,'linear');
co_flux_interp_8(:,co)=interp1(wave(857:883),co_flux_8(857:883,co),wave_interp,'linear');
co_flux_interp_9(:,co)=interp1(wave(857:883),co_flux_9(857:883,co),wave_interp,'linear');
co_flux_interp_10(:,co)=interp1(wave(857:883),co_flux_10(857:883,co),wave_interp,'linear');
co_flux_interp_11(:,co)=interp1(wave(857:883),co_flux_11(857:883,co),wave_interp,'linear');
co_flux_interp_12(:,co)=interp1(wave(857:883),co_flux_12(857:883,co),wave_interp,'linear');
co_flux_interp_13(:,co)=interp1(wave(857:883),co_flux_13(857:883,co),wave_interp,'linear');
%--------

%Dco index calculations
CO1(co)=((sum(co_flux_interp_1(1011:1101,co))+sum(co_flux_interp_1(1261:1321,co)))/...
    ((1101-1011)+(1321-1261)))/...
((sum(co_flux_interp_1(1431:1561,co)))/(1561-1431));
CO2(co)=((sum(co_flux_interp_2(1011:1101,co))+sum(co_flux_interp_2...
    (1261:1321,co)))/((1101-1011)+(1321-1261)))/...
    ((sum(co_flux_interp_2(1431:1561,co)))/(1561-1431));
CO3(co)=((sum(co_flux_interp_3(1011:1101,co))+sum(co_flux_interp_3...
    (1261:1321,co)))/((1101-1011)+(1321-1261)))/...
    ((sum(co_flux_interp_3(1431:1561,co)))/(1561-1431));
CO4(co)=((sum(co_flux_interp_4(1011:1101,co))+sum(co_flux_interp_4...
    (1261:1321,co)))/((1101-1011)+(1321-1261)))/...
    ((sum(co_flux_interp_4(1431:1561,co)))/(1561-1431));
CO5(co)=((sum(co_flux_interp_5(1011:1101,co))+sum(co_flux_interp_5...
    (1261:1321,co)))/((1101-1011)+(1321-1261)))/...
    ((sum(co_flux_interp_5(1431:1561,co)))/(1561-1431));
CO6(co)=((sum(co_flux_interp_6(1011:1101,co))+sum(co_flux_interp_6...
    (1261:1321,co)))/((1101-1011)+(1321-1261)))/...
```

```
      ((sum(co_flux_interp_6(1431:1561,co)))/(1561-1431));
CO7(co)=((sum(co_flux_interp_7(1011:1101,co))+sum(co_flux_interp_7...
    (1261:1321,co)))/((1101-1011)+(1321-1261)))/...
    ((sum(co_flux_interp_7(1431:1561,co)))/(1561-1431));
CO8(co)=((sum(co_flux_interp_8(1011:1101,co))+sum(co_flux_interp_8...
    (1261:1321,co)))/((1101-1011)+(1321-1261)))/...
    ((sum(co_flux_interp_8(1431:1561,co)))/(1561-1431));
CO9(co)=((sum(co_flux_interp_9(1011:1101,co))+sum(co_flux_interp_9...
    (1261:1321,co)))/((1101-1011)+(1321-1261)))/...
    ((sum(co_flux_interp_9(1431:1561,co)))/(1561-1431));
CO10(co)=((sum(co_flux_interp_10(1011:1101,co))+sum(co_flux_interp_10...
    (1261:1321,co)))/((1101-1011)+(1321-1261)))/...
    ((sum(co_flux_interp_10(1431:1561,co)))/(1561-1431));
CO11(co)=((sum(co_flux_interp_11(1011:1101,co))+sum(co_flux_interp_11...
    (1261:1321,co)))/((1101-1011)+(1321-1261)))/...
    ((sum(co_flux_interp_11(1431:1561,co)))/(1561-1431));
CO12(co)=((sum(co_flux_interp_12(1011:1101,co))+sum(co_flux_interp_12...
    (1261:1321,co)))/((1101-1011)+(1321-1261)))/...
    ((sum(co_flux_interp_12...
    (1431:1561,co)))/(1561-1431));
CO13(co)=((sum(co_flux_interp_13(1011:1101,co))+sum(co_flux_interp_13...
    (1261:1321,co)))/((1101-1011)+(1321-1261)))/...
    ((sum(co_flux_interp_13(1431:1561,co)))/(1561-1431));

%K&G CO_KG
% ---
% CO1(co)=-2.5.*log10((sum(co_flux_interp_1(1751:2551,co)))/...
% (sum(co_flux_interp_1(1:1101,co))))-CO_0;
% CO2(co)=-2.5.*log10((sum(co_flux_interp_2(1751:2551,co)))/...
% (sum(co_flux_interp_2(1:1101,co))))-CO_0;
% CO3(co)=-2.5.*log10((sum(co_flux_interp_3(1751:2551,co)))/...
% (sum(co_flux_interp_3(1:1101,co))))-CO_0;
% CO4(co)=-2.5.*log10((sum(co_flux_interp_4(1751:2551,co)))/...
% (sum(co_flux_interp_4(1:1101,co))))-CO_0;
% CO5(co)=-2.5.*log10((sum(co_flux_interp_5(1751:2551,co)))/...
% (sum(co_flux_interp_5(1:1101,co))))-CO_0;
% CO6(co)=-2.5.*log10((sum(co_flux_interp_6(1751:2551,co)))/...
% (sum(co_flux_interp_6(1:1101,co))))-CO_0;
% CO7(co)=-2.5.*log10((sum(co_flux_interp_7(1751:2551,co)))/...
```

```matlab
% (sum(co_flux_interp_7(1:1101,co))))-CO_0;
% CO8(co)=-2.5.*log10((sum(co_flux_interp_8(1751:2551,co)))/...
% (sum(co_flux_interp_8(1:1101,co))))-CO_0;
% CO9(co)=-2.5.*log10((sum(co_flux_interp_9(1751:2551,co)))/...
% (sum(co_flux_interp_9(1:1101,co))))-CO_0;
% CO10(co)=-2.5.*log10((sum(co_flux_interp_10(1751:2551,co)))/...
% (sum(co_flux_interp_10(1:1101,co))))-CO_0;
% CO11(co)=-2.5.*log10((sum(co_flux_interp_11(1751:2551,co)))/...
% (sum(co_flux_interp_11(1:1101,co))))-CO_0;
% CO12(co)=-2.5.*log10((sum(co_flux_interp_12(1751:2551,co)))/...
% (sum(co_flux_interp_12(1:1101,co))))-CO_0;
% CO13(co)=-2.5.*log10((sum(co_flux_interp_13(1751:2551,co)))/...
% (sum(co_flux_interp_13(1:1101,co))))-CO_0;
%-------
%%%%
end

%plot CO values
%define age vector
age_co=[1 2 3 4 5 6 7 8 9 10 12 14 16 18 20 25 30 35 40 45 50 60 70 80 90 100 120 140 160 180 200 ...
    250 300 350 400 450 500 600 700 800 900 1000 1200 1400 1600 1800 2000 2500 3000 3500 4000 ...
    4500 5000 6000 7000 8000 9000 10000 11000 12000 13000 14000 15000 16000 17000 18000 19000 ...
    20000].*1e6;

figure(3)
hold on
area([10000 14000].*1e6,[1.4 1.4],'LineStyle','none',...
    'FaceColor',[0.803921568627451 0.87843137254902 0.968627450980392])

co1=plot(age_co,CO1,'m','linewidth',1.5)
co2=plot(age_co,CO2,'k','linewidth',1.5)
co3=plot(age_co,CO3,'c','linewidth',1.5)
co4=plot(age_co,CO4,'g','linewidth',1.5)
co5=plot(age_co,CO5,'b','linewidth',1.5)
co6=plot(age_co,CO6,'r','linewidth',1.5)
%co7=plot(age_co,CO7,'m--','linewidth',1.5)
co8=plot(age_co,CO8,'m--','linewidth',1.5)
co9=plot(age_co,CO9,'b--','linewidth',1.5)
co10=plot(age_co,CO10,'r--','linewidth',1.5)
```

```
co11=plot(age_co,CO11,'k--','linewidth',1.5)
co12=plot(age_co,CO12,'c--','linewidth',1.5)
co13=plot(age_co,CO13,'g--','linewidth',1.5)

Xlim([0 2e10])
Ylim([1.1 1.24])
xlabel('Age [yr]','FontSize',16)
ylabel('D_{CO}','FontSize',16)
legend([co1 co5 co6 co8 co9 co10 co2 co3 co4 co11 co12 co13],'1.35 Z=0.020 SSP','1.35 Z=0.016 ...
    SSP',...
    '1.35 Z=0.024 SSP','1.35 Z=0.020 SFR','1.35 Z=0.016 SFR','1.35 Z=0.024 SFR','2.0 Z=0.020 SSP',...
    '2.0 Z=0.016 SSP','2.0 Z=0.024 SSP','2.0 Z=0.020 SFR','2.0 Z=0.016 SFR','2.0 Z=0.024 SFR')

legend1 = legend(gca,'show');
set(legend1,'Location','NorthEastOutside','FontSize',12);

set(gca,'YTickLabel',{'','1.02','1.04','1.06','1.08','1.1','1.12','1.14','1.16','1.18','1.2','1.22',...
    '1.24','1.26','1.28',''},...
    'YTick',[1 1.02 1.04 1.06 1.08 1.1 1.12 1.14 1.16 1.18 1.2 1.22 1.24 1.26 1.28 1.3],...
    'Xtick',[10^6 10^7 10^8 10^9 10^10],...
    'XScale','log',...
    'XMinorTick','on',...
    'Layer','top',...
    'FontSize',16,...
    'box','on');

figure(4)
hold on

[s20fill,msg]=jbfill(age_co,CO3,CO13,[0.729411780834198 0.831372559070587 0.95686274766922],...
    [0.729411780834198 0.831372559070587 0.95686274766922],1,1);
[s13fill1,msg]=jbfill(age_co,CO5,CO10,[1 0.4 0.4],[1 0.4 0.4],1,1);
[s13fill1,msg]=jbfill(age_co,CO13,CO10,[1 0.9 0.9],[1 0.9 0.9],1,1);

hold off
figure(4)
hold on

co1=plot(age_co,CO1,'m','linewidth',1.5)
```

```matlab
co2=plot(age_co,CO2,'k','linewidth',1.5)
co3=plot(age_co,CO3,'c','linewidth',1.5)
co4=plot(age_co,CO4,'g','linewidth',1.5)
co5=plot(age_co,CO5,'b','linewidth',1.5)
co6=plot(age_co,CO6,'r','linewidth',1.5)
%co7=plot(age_co,CO7,'m--','linewidth',1.5)
co8=plot(age_co,CO8,'m--','linewidth',1.5)
co9=plot(age_co,CO9,'b--','linewidth',1.5)
co10=plot(age_co,CO10,'r--','linewidth',1.5)
co11=plot(age_co,CO11,'k--','linewidth',1.5)
co12=plot(age_co,CO12,'c--','linewidth',1.5)
co13=plot(age_co,CO13,'g--','linewidth',1.5)




Xlim([10 14]*1e9)
Ylim([1.164988238172306 1.19152969962625617])
xlabel('Age [yr]','FontSize',16)
ylabel('D_{CO}','FontSize',16)
%title('CO-index as a function of age, remaining star formation')
legend([co1 co5 co6 co8 co9 co10 co2 co3 co4 co11 co12 co13],'1.35 Z=0.020 SSP','1.35 Z=0.016 ...
   SSP',...
    '1.35 Z=0.024 SSP','1.35 Z=0.020 SFR','1.35 Z=0.016 SFR','1.35 Z=0.024 SFR','2.0 Z=0.020 SSP',...
    '2.0 Z=0.016 SSP','2.0 Z=0.024 SSP','2.0 Z=0.020 SFR','2.0 Z=0.016 SFR','2.0 Z=0.024 SFR')

legend1 = legend(gca,'show');
set(legend1,'Location','NorthEastOutside','FontSize',12);

set(gca,'XMinorTick','on',...
    'Layer','top',...
    'FontSize',16,...
    'box','on');

figure(5)
hold on

[s20fill,msg]=jbfill(age_co,CO3+0.03725,CO13+0.03725,[0.729411780834198 0.831372559070587 ...
   0.95686274766922],...
```

```
      [0.729411780834198 0.831372559070587 0.95686274766922],1,1);
[s20fill,msg]=jbfill(age_co,CO12+0.03725,CO13+0.03725,[0.729411780834198 0.831372559070587 ...
    0.95686274766922],...
      [0.729411780834198 0.831372559070587 0.95686274766922],1,1);
[s13fill1,msg]=jbfill(age_co,CO5+0.03725,CO10+0.03725,[1 0.4 0.4],[1 0.4 0.4],1,1);
[s13fill1,msg]=jbfill(age_co,CO13+0.03725,CO10+0.03725,[1 0.9 0.9],[1 0.9 0.9],1,1);
[s13fill1,msg]=jbfill(age_co(1:51),CO13(1:51)+0.03725,CO5(1:51)+0.03725,[0.729411780834198 ...
    0.831372559070587...
     0.95686274766922],[0.729411780834198 0.831372559070587 0.95686274766922],1,1);
[s13fill1,msg]=jbfill(age_co(1:53),CO5(1:53)+0.03725,CO4(1:53)+0.03725,[1 0.4 0.4],[1 0.4 0.4],1,1);

hold off
figure(5)
hold on

co1=plot(age_co,CO1+0.03725,'m','linewidth',1.5)
co2=plot(age_co,CO2+0.03725,'k','linewidth',1.5)
co3=plot(age_co,CO3+0.03725,'c','linewidth',1.5)
co4=plot(age_co,CO4+0.03725,'g','linewidth',1.5)
co5=plot(age_co,CO5+0.03725,'b','linewidth',1.5)
co6=plot(age_co,CO6+0.03725,'r','linewidth',1.5)
%co7=plot(age_co,CO7,'m--','linwidth',1.5)
co8=plot(age_co,CO8+0.03725,'m--','linewidth',1.5)
co9=plot(age_co,CO9+0.03725,'b--','linewidth',1.5)
co10=plot(age_co,CO10+0.03725,'r--','linewidth',1.5)
co11=plot(age_co,CO11+0.03725,'k--','linewidth',1.5)
co12=plot(age_co,CO12+0.03725,'c--','linewidth',1.5)
co13=plot(age_co,CO13+0.03725,'g--','linewidth',1.5)


DCO=[1.2028 1.2196 1.2107 1.2314 1.2258 1.2136 1.1952 1.2083 1.2012];
ee=[0.0016 0.0025 0.0022 0.0019 0.0015 0.0006 0.0006 0.0005 0.0004];
ll=length(DCO);
%agemarmol=[(1+(rand(ll,1)/2))*1e10];
agemarmol=[5.8 5 12.4451 5.9 3.4 7.7 1.5 6.6 7.9].*1e9;

errorbar(agemarmol,DCO,ee,'k+','linewidth',1.5)

ehoriz=agemarmol.*0.2;
```

```
herr=herrorbar(agemarmol,DCO,ehoriz);
set(herr(2),'linewidth',1.5,'linestyle','none')
set(herr(1),'linewidth',1.5,'linestyle','-','color','black')

co14=plot(10^10.095,1.2107,'linewidth',10,'MarkerSize',14,'Marker','*','LineWidth',2,'LineStyle',...
    'none','Color','magenta');

DCOS=[1.2258 1.1952 1.2083];
eeS=[0.0015 0.0006 0.0005];
agemarmolS=[3.4 1.5 6.6].*1e9;
co15=plot(agemarmolS,DCOS,'linewidth',8,'MarkerSize',12,'Marker','o','LineWidth',2,'LineStyle',...
    'none','Color','red');

Xlim([1 15]*1e9)
Ylim([1.19 1.235])
xlabel('Age [yr]','FontSize',16)
ylabel('D_{CO}','FontSize',16)
legend([co1 co5 co6 co8 co9 co10 co2 co3 co4 co11 co12 co13 co14 co15],'1.35 Z=0.020 SSP','1.35 ...
    Z=0.016 SSP',...
    '1.35 Z=0.024 SSP','1.35 Z=0.020 SFR','1.35 Z=0.016 SFR','1.35 Z=0.024 SFR','2.0 Z=0.020 ...
        SSP','2.0 Z=0.016 SSP',...
    '2.0 Z=0.024 SSP','2.0 Z=0.020 SFR','2.0 Z=0.016 SFR','2.0 Z=0.024 SFR','NGC 4261','S0 galaxies')

legend1 = legend(gca,'show');
set(legend1,'FontSize',12);
set(legend1,'Location','NorthEastOutside','FontSize',12);

set(gca,'XMinorTick','on',...
    'Layer','top',...
    'FontSize',16,...
    'box','on');
figure(6)
hold on

[s20fill,msg]=jbfill(age_co,CO3+0.03725-0.00975,CO13+0.03725-0.00975,...
    [0.729411780834198 0.831372559070587 0.95686274766922],...
    [0.729411780834198 0.831372559070587 0.95686274766922],1,1);
[s20fill,msg]=jbfill(age_co,CO12+0.03725-0.00975,CO13+0.03725-0.00975,...
    [0.729411780834198 0.831372559070587 0.95686274766922],...
```

```matlab
    [0.729411780834198 0.831372559070587 0.95686274766922],1,1);
[s13fill1,msg]=jbfill(age_co,CO5+0.03725-0.00975,CO10+0.03725-0.00975,...
    [1 0.4 0.4],[1 0.4 0.4],1,1);
[s13fill1,msg]=jbfill(age_co,CO13+0.03725-0.00975,CO10+0.03725-0.00975,...
    [1 0.9 0.9],[1 0.9 0.9],1,1);
[s13fill1,msg]=jbfill(age_co(1:51),CO13(1:51)+0.03725-0.00975,CO5(1:51)+...
    0.03725-0.00975,[0.729411780834198 0.831372559070587 0.95686274766922],...
    [0.729411780834198 0.831372559070587 0.95686274766922],1,1);
[s13fill1,msg]=jbfill(age_co(1:53),CO5(1:53)+0.03725-0.00975,CO4(1:53)+...
    0.03725-0.00975,[1 0.4 0.4],[1 0.4 0.4],1,1);

hold off
figure(6)
hold on

co1=plot(age_co,CO1+0.03725-0.00975,'m','linewidth',1.5)
co2=plot(age_co,CO2+0.03725-0.00975,'k','linewidth',1.5)
co3=plot(age_co,CO3+0.03725-0.00975,'c','linewidth',1.5)
co4=plot(age_co,CO4+0.03725-0.00975,'g','linewidth',1.5)
co5=plot(age_co,CO5+0.03725-0.00975,'b','linewidth',1.5)
co6=plot(age_co,CO6+0.03725-0.00975,'r','linewidth',1.5)
%co7=plot(age_co,CO7,'m--','linwidth',1.5)
co8=plot(age_co,CO8+0.03725-0.00975,'m--','linewidth',1.5)
co9=plot(age_co,CO9+0.03725-0.00975,'b--','linewidth',1.5)
co10=plot(age_co,CO10+0.03725-0.00975,'r--','linewidth',1.5)
co11=plot(age_co,CO11+0.03725-0.00975,'k--','linewidth',1.5)
co12=plot(age_co,CO12+0.03725-0.00975,'c--','linewidth',1.5)
co13=plot(age_co,CO13+0.03725-0.00975,'g--','linewidth',1.5)

DCO=[1.2028 1.2196 1.2107 1.2314 1.2258 1.2136 1.1952 1.2083 1.2012];
ee=[0.0016 0.0025 0.0022 0.0019 0.0015 0.0006 0.0006 0.0005 0.0004];
ll=length(DCO);
%agemarmol=[(1+(rand(ll,1)/2))*1e10];
agemarmol=[5.8 5 12.4451 5.9 3.4 7.7 1.5 6.6 7.9].*1e9;

errorbar(agemarmol,DCO,ee,'k+','linewidth',1.5)

ehoriz=agemarmol.*0.2;
herr=herrorbar(agemarmol,DCO,ehoriz);
```

```matlab
set(herr(2),'linewidth',1.5,'linestyle','none')
set(herr(1),'linewidth',1.5,'linestyle','-','color','black')


co14=plot(10^10.095,1.2107,'linewidth',10,'MarkerSize',14,'Marker','*','LineWidth',2,'LineStyle',...
    'none','Color','magenta');


DCOS=[1.2258 1.1952 1.2083];
eeS=[0.0015 0.0006 0.0005];
agemarmolS=[3.4 1.5 6.6].*1e9;
co15=plot(agemarmolS,DCOS,'linewidth',8,'MarkerSize',12,'Marker','o','LineWidth',2,'LineStyle',...
    'none','Color','red');



Xlim([1 15]*1e9)
Ylim([1.185 1.235])
xlabel('Age [yr]','FontSize',16)
ylabel('D_{CO}','FontSize',16)
%title('CO-index as a function of age, remaining star formation')
legend([co1 co5 co6 co8 co9 co10 co2 co3 co4 co11 co12 co13 co14 co15],'1.35 Z=0.020 SSP','1.35 ...
    Z=0.016 SSP',...
    '1.35 Z=0.024 SSP','1.35 Z=0.020 SFR','1.35 Z=0.016 SFR','1.35 Z=0.024 SFR','2.0 Z=0.020 ...
        SSP','2.0 Z=0.016 SSP'...
    ,'2.0 Z=0.024 SSP','2.0 Z=0.020 SFR','2.0 Z=0.016 SFR','2.0 Z=0.024 SFR','NGC 4261','S0 ...
        galaxies')

legend1 = legend(gca,'show');
set(legend1,'FontSize',12);



set(legend1,'Location','NorthEastOutside','FontSize',12);

set(gca,'XMinorTick','on',...
    'Layer','top',...
    'FontSize',16,...
    'box','on');
```

A.2. M/L ratio and V-I_C color index

```
%extracting M/L and V-I_C data from pegase .dat files

%clear
close all
clear all


%%% initiate vectors
time=[];
Mgal=[];
M=[];
MWD=[];
MBHNS=[];
LVLVsol=[];
VIC=[];
VIJ=[];
%%%

%read files
[timer, Mgalr, Mr, MWDr, MBHNSr, Msubr, Mgasr, Zgasr, zmassr, zLbolr] = ...
    textread('SSPs/sal13c.dat','%f %f %f %f %f %f %f %f %f %f',68,'headerlines', 33,'expchars','E');
time=[time timer];
Mgal=[Mgal Mgalr];
M=[M Mr];
MWD=[MWD MWDr];
MBHNS=[MBHNS MBHNSr];
[timer, Mgalr, Mr, MWDr, MBHNSr, Msubr, Mgasr, Zgasr, zmassr, zLbolr] = ...
    textread('SSPs/sal20c.dat','%f %f %f %f %f %f %f %f %f %f',68,'headerlines', 33,'expchars','E');
Mgal=[Mgal Mgalr];
M=[M Mr];
MWD=[MWD MWDr];
MBHNS=[MBHNS MBHNSr];
[timer, Mgalr, Mr, MWDr, MBHNSr, Msubr, Mgasr, Zgasr, zmassr, zLbolr] = ...
    textread('SSPs/kroupc.dat','%f %f %f %f %f %f %f %f %f %f',68,'headerlines', 33,'expchars','E');
Mgal=[Mgal Mgalr];
```

```
M=[M Mr];
MWD=[MWD MWDr];
MBHNS=[MBHNS MBHNSr];
[timer, Mgalr, Mr, MWDr, MBHNSr, Msubr, Mgasr, Zgasr, zmassr, zLbolr] = ...
    textread('SSPs/kroupa01c.dat','%f %f %f %f %f %f %f %f %f %f',68,'headerlines', ...
    33,'expchars','E');
Mgal=[Mgal Mgalr];
M=[M Mr];
MWD=[MWD MWDr];
MBHNS=[MBHNS MBHNSr];
[timer, Mgalr, Mr, MWDr, MBHNSr, Msubr, Mgasr, Zgasr, zmassr, zLbolr] = ...
    textread('SSPs/s20c08.dat','%f %f %f %f %f %f %f %f %f %f',68,'headerlines', 33,'expchars','E');
Mgal=[Mgal Mgalr];
M=[M Mr];
MWD=[MWD MWDr];
MBHNS=[MBHNS MBHNSr];
[timer, Mgalr, Mr, MWDr, MBHNSr, Msubr, Mgasr, Zgasr, zmassr, zLbolr] = ...
    textread('SSPs/s20c12.dat','%f %f %f %f %f %f %f %f %f %f',68,'headerlines', 33,'expchars','E');
Mgal=[Mgal Mgalr];
M=[M Mr];
MWD=[MWD MWDr];
MBHNS=[MBHNS MBHNSr];
[timer, Mgalr, Mr, MWDr, MBHNSr, Msubr, Mgasr, Zgasr, zmassr, zLbolr] = ...
    textread('SSPs/s13c08.dat','%f %f %f %f %f %f %f %f %f %f',68,'headerlines', 33,'expchars','E');
Mgal=[Mgal Mgalr];
M=[M Mr];
MWD=[MWD MWDr];
MBHNS=[MBHNS MBHNSr];
[timer, Mgalr, Mr, MWDr, MBHNSr, Msubr, Mgasr, Zgasr, zmassr, zLbolr] = ...
    textread('SSPs/s13c12.dat','%f %f %f %f %f %f %f %f %f %f',68,'headerlines', 33,'expchars','E');
Mgal=[Mgal Mgalr];
M=[M Mr];
MWD=[MWD MWDr];
MBHNS=[MBHNS MBHNSr];
[timer, Mgalr, Mr, MWDr, MBHNSr, Msubr, Mgasr, Zgasr, zmassr, zLbolr] = ...
    textread('SSPs/13crz1.dat','%f %f %f %f %f %f %f %f %f %f',68,'headerlines', 35,'expchars','E');
Mgal=[Mgal Mgalr];
M=[M Mr];
MWD=[MWD MWDr];
```

```matlab
MBHNS=[MBHNS MBHNSr];
[timer, Mgalr, Mr, MWDr, MBHNSr, Msubr, Mgasr, Zgasr, zmassr, zLbolr] = ...
    textread('SSPs/13crz8.dat','%f %f %f %f %f %f %f %f %f %f',68,'headerlines', 35,'expchars','E');
Mgal=[Mgal Mgalr];
M=[M Mr];
MWD=[MWD MWDr];
MBHNS=[MBHNS MBHNSr];
[timer, Mgalr, Mr, MWDr, MBHNSr, Msubr, Mgasr, Zgasr, zmassr, zLbolr] = ...
    textread('SSPs/13crz2.dat','%f %f %f %f %f %f %f %f %f %f',68,'headerlines', 35,'expchars','E');
Mgal=[Mgal Mgalr];
M=[M Mr];
MWD=[MWD MWDr];
MBHNS=[MBHNS MBHNSr];
[timer, Mgalr, Mr, MWDr, MBHNSr, Msubr, Mgasr, Zgasr, zmassr, zLbolr] = ...
    textread('SSPs/20crz1.dat','%f %f %f %f %f %f %f %f %f %f',68,'headerlines', 35,'expchars','E');
Mgal=[Mgal Mgalr];
M=[M Mr];
MWD=[MWD MWDr];
MBHNS=[MBHNS MBHNSr];
[timer, Mgalr, Mr, MWDr, MBHNSr, Msubr, Mgasr, Zgasr, zmassr, zLbolr] = ...
    textread('SSPs/20crz8.dat','%f %f %f %f %f %f %f %f %f %f',68,'headerlines', 35,'expchars','E');
Mgal=[Mgal Mgalr];
M=[M Mr];
MWD=[MWD MWDr];
MBHNS=[MBHNS MBHNSr];
[timer, Mgalr, Mr, MWDr, MBHNSr, Msubr, Mgasr, Zgasr, zmassr, zLbolr] = ...
    textread('SSPs/20crz2.dat','%f %f %f %f %f %f %f %f %f %f',68,'headerlines', 35,'expchars','E');
Mgal=[Mgal Mgalr];
M=[M Mr];
MWD=[MWD MWDr];
MBHNS=[MBHNS MBHNSr];


%skip to next datablock and read luminosity data
[time, nLymcont , LHa  , WHa ,  LHb ,  WHb , LBLBsol, LVLVsolr ,  D4000] = ...
    textread('SSPs/sal13c.dat','%f %f %f %f %f %f %f %f %f',68,'headerlines', ...
    33+68+1+68+1,'expchars','E');
LVLVsol=[LVLVsol LVLVsolr];
[time, nLymcont ,  LHa   , WHa   , LHb  ,  WHb , LBLBsol ,LVLVsolr  , D4000] = ...
```

```matlab
    textread('SSPs/sal20c.dat','%f %f %f %f %f %f %f %f %f',68,'headerlines', ...
    33+68+1+68+1,'expchars','E');
LVLVsol=[LVLVsol LVLVsolr];
[time, nLymcont ,  LHa  , WHa  , LHb  ,  WHb , LBLBsol ,LVLVsolr  , D4000] = ...
    textread('SSPs/kroupc.dat','%f %f %f %f %f %f %f %f %f',68,'headerlines', ...
    33+68+1+68+1,'expchars','E');
LVLVsol=[LVLVsol LVLVsolr];
[time, nLymcont ,  LHa  , WHa  , LHb  ,  WHb , LBLBsol ,LVLVsolr  , D4000] = ...
    textread('SSPs/kroupa01c.dat','%f %f %f %f %f %f %f %f %f',68,'headerlines', ...
    33+68+1+68+1,'expchars','E');
LVLVsol=[LVLVsol LVLVsolr];
[time, nLymcont ,  LHa  , WHa  , LHb  ,  WHb , LBLBsol ,LVLVsolr  , D4000] = ...
    textread('SSPs/s20c08.dat','%f %f %f %f %f %f %f %f %f',68,'headerlines', ...
    33+68+1+68+1,'expchars','E');
LVLVsol=[LVLVsol LVLVsolr];
[time, nLymcont ,  LHa  , WHa  , LHb  ,  WHb , LBLBsol ,LVLVsolr  , D4000] = ...
    textread('SSPs/s20c12.dat','%f %f %f %f %f %f %f %f %f',68,'headerlines', ...
    33+68+1+68+1,'expchars','E');
LVLVsol=[LVLVsol LVLVsolr];
[time, nLymcont ,  LHa  , WHa  , LHb  ,  WHb , LBLBsol ,LVLVsolr  , D4000] = ...
    textread('SSPs/s13c08.dat','%f %f %f %f %f %f %f %f %f',68,'headerlines', ...
    33+68+1+68+1,'expchars','E');
LVLVsol=[LVLVsol LVLVsolr];
[time, nLymcont ,  LHa  , WHa  , LHb  ,  WHb , LBLBsol ,LVLVsolr  , D4000] = ...
    textread('SSPs/s13c12.dat','%f %f %f %f %f %f %f %f %f',68,'headerlines', ...
    33+68+1+68+1,'expchars','E');
LVLVsol=[LVLVsol LVLVsolr];
[time, nLymcont ,  LHa  , WHa  , LHb  ,  WHb , LBLBsol ,LVLVsolr  , D4000] = ...
    textread('SSPs/13crz1.dat','%f %f %f %f %f %f %f %f %f',68,'headerlines', ...
    35+68+1+68+1,'expchars','E');
LVLVsol=[LVLVsol LVLVsolr];
[time, nLymcont ,  LHa  , WHa  , LHb  ,  WHb , LBLBsol ,LVLVsolr  , D4000] = ...
    textread('SSPs/13crz8.dat','%f %f %f %f %f %f %f %f %f',68,'headerlines', ...
    35+68+1+68+1,'expchars','E');
LVLVsol=[LVLVsol LVLVsolr];
[time, nLymcont ,  LHa  , WHa  , LHb  ,  WHb , LBLBsol ,LVLVsolr  , D4000] = ...
    textread('SSPs/13crz2.dat','%f %f %f %f %f %f %f %f %f',68,'headerlines', ...
    35+68+1+68+1,'expchars','E');
LVLVsol=[LVLVsol LVLVsolr];
```

```matlab
[time, nLymcont ,  LHa   ,  WHa   ,  LHb  ,   WHb , LBLBsol ,LVLVsolr  , D4000] = ...
    textread('SSPs/20crz1.dat','%f %f %f %f %f %f %f %f %f',68,'headerlines', ...
    35+68+1+68+1,'expchars','E');
LVLVsol=[LVLVsol LVLVsolr];
[time, nLymcont ,  LHa   ,  WHa   ,  LHb  ,   WHb , LBLBsol ,LVLVsolr  , D4000] = ...
    textread('SSPs/20crz8.dat','%f %f %f %f %f %f %f %f %f',68,'headerlines', ...
    35+68+1+68+1,'expchars','E');
LVLVsol=[LVLVsol LVLVsolr];
[time, nLymcont ,  LHa   ,  WHa   ,  LHb  ,   WHb , LBLBsol ,LVLVsolr  , D4000] = ...
    textread('SSPs/20crz2.dat','%f %f %f %f %f %f %f %f %f',68,'headerlines', ...
    35+68+1+68+1,'expchars','E');
LVLVsol=[LVLVsol LVLVsolr];

%read color data
[timer  , Mbolr   ,  Vr   ,  UBr  ,  BVr  ,   VKr    , VRCr   , VICr  ,  JHr  ,   HKr] = ...
    textread('SSPs/sal13c.dat','%f %f %f %f %f %f %f %f %f %f',68,'headerlines', ...
    33+68+1+68+1+68+1,'expchars','E');
VIC=[VIC VICr];
[timer  ,  Mbolr   ,   Vr   ,   UBr  ,   BVr  ,   VKr   ,   VRCr   ,  VICr   ,  JHr   ,   HKr] = ...
    textread('SSPs/sal20c.dat','%f %f %f %f %f %f %f %f %f %f',68,'headerlines', ...
    33+68+1+68+1+68+1,'expchars','E');
VIC=[VIC VICr];
[timer  ,  Mbolr   ,   Vr   ,   UBr  ,   BVr  ,   VKr   ,   VRCr   ,  VICr   ,  JHr   ,   HKr] = ...
    textread('SSPs/s20c12.dat','%f %f %f %f %f %f %f %f %f %f',68,'headerlines', ...
    33+68+1+68+1+68+1,'expchars','E');
VIC=[VIC VICr];
[timer  ,  Mbolr   ,   Vr   ,   UBr  ,   BVr  ,   VKr   ,   VRCr   ,  VICr   ,  JHr   ,   HKr] = ...
    textread('SSPs/s20c08.dat','%f %f %f %f %f %f %f %f %f %f',68,'headerlines', ...
    33+68+1+68+1+68+1,'expchars','E');
VIC=[VIC VICr];
[timer  ,  Mbolr   ,   Vr   ,   UBr  ,   BVr  ,   VKr   ,   VRCr   ,  VICr   ,  JHr   ,   HKr] = ...
    textread('SSPs/s13c12.dat','%f %f %f %f %f %f %f %f %f %f',68,'headerlines', ...
    33+68+1+68+1+68+1,'expchars','E');
VIC=[VIC VICr];
[timer  ,  Mbolr   ,   Vr   ,   UBr  ,   BVr  ,   VKr   ,   VRCr   ,  VICr   ,  JHr   ,   HKr] = ...
    textread('SSPs/s13c08.dat','%f %f %f %f %f %f %f %f %f %f',68,'headerlines', ...
    33+68+1+68+1+68+1,'expchars','E');
VIC=[VIC VICr];
```

```matlab
%read  color data
[ timer ,   KLr  ,   LMr  ,  VRJr  ,  VIJr   , JKVr  , UKJKr  , JKFKr   ,FKNKr  ,Vr2000] = ...
   textread('SSPs/sal13c.dat','%f %f %f %f %f %f %f %f %f %f',68,'headerlines', ...
   33+68+1+68+1+68+1+68+1,'expchars','E');
VIJ=[VIJ VIJr];
[ timer ,   KLr  ,   LMr  ,  VRJr  ,  VIJr   , JKVr  , UKJKr  , JKFKr   ,FKNKr  ,Vr2000] = ...
   textread('SSPs/sal20c.dat','%f %f %f %f %f %f %f %f %f %f',68,'headerlines', ...
   33+68+1+68+1+68+1+68+1,'expchars','E');
VIJ=[VIJ VIJr];
[ timer ,   KLr  ,   LMr  ,  VRJr  ,  VIJr   , JKVr  , UKJKr  , JKFKr   ,FKNKr  ,Vr2000] = ...
   textread('SSPs/s20c12.dat','%f %f %f %f %f %f %f %f %f %f',68,'headerlines', ...
   33+68+1+68+1+68+1+68+1,'expchars','E');
VIJ=[VIJ VIJr];
[ timer ,   KLr  ,   LMr  ,  VRJr  ,  VIJr   , JKVr  , UKJKr  , JKFKr   ,FKNKr  ,Vr2000] = ...
   textread('SSPs/s20c08.dat','%f %f %f %f %f %f %f %f %f %f',68,'headerlines', ...
   33+68+1+68+1+68+1+68+1,'expchars','E');
VIJ=[VIJ VIJr];
[ timer ,   KLr  ,   LMr  ,  VRJr  ,  VIJr   , JKVr  , UKJKr  , JKFKr   ,FKNKr  ,Vr2000] = ...
   textread('SSPs/s13c12.dat','%f %f %f %f %f %f %f %f %f %f',68,'headerlines', ...
   33+68+1+68+1+68+1+68+1,'expchars','E');
VIJ=[VIJ VIJr];
[ timer ,   KLr  ,   LMr  ,  VRJr  ,  VIJr   , JKVr  , UKJKr  , JKFKr   ,FKNKr  ,Vr2000] = ...
   textread('SSPs/s13c08.dat','%f %f %f %f %f %f %f %f %f %f',68,'headerlines', ...
   33+68+1+68+1+68+1+68+1,'expchars','E');
VIJ=[VIJ VIJr];

%---
%file reading done
%---


%%%%
%color index and M/L ratio calculations and plots

%Calculate Mass to light ratios

ML=(M+MWD+MBHNS)./LVLVsol;

%define age vector
age=[1 2 3 4 5 6 7 8 9 10 12 14 16 18 20 25 30 35 40 45 50 60 70 80 90 100 120 140 160 180 200 ...
```

```matlab
    250 300 350 400 450 500 600 700 800 900 1000 1200 1400 1600 1800 2000 2500 3000 3500 4000 ...
    4500 5000 6000 7000 8000 9000 10000 11000 12000 13000 14000 15000 16000 17000 18000 19000 ...
    20000].*1e6;

%plot M/LVLVsol ratio
figure(1)
hold on

[s20fill,msg]=jbfill(log10(age),ML(:,6)',ML(:,13)',[0.729411780834198 0.831372559070587 ...
    0.95686274766922],...
     [0.729411780834198 0.831372559070587 0.95686274766922],1,1);
[s13fill1,msg]=jbfill(log10(age),ML(:,8)',ML(:,10)',[1 0.8 0.8],[1 0.8 0.8],1,1);
[s13fill2,msg]=jbfill(log10(age),ML(:,8)',ML(:,7)',[1 0.8 0.8],[1 0.8 0.8],1,1);

hold off

figure(1)
hold on

ML1=plot(log10(age),(ML(:,1)),'Color',[0.749019622802734 0 0.749019622802734],'linewidth',2)
ML2=plot(log10(age),(ML(:,2)),'k','linewidth',2)
ML3=plot(log10(age),(ML(:,4)),'Color',[0.0431372560560703 0.517647087574005 ...
    0.780392169952393],'linewidth',2)


Xlim([log10(age(20)) log10(age(end))])
Ylim([-1.5 22])
xlabel('log Age','FontSize',16)
ylabel('M/L_V','FontSize',16)
title('a)','FontSize',16)
legend([ML1 ML2 ML3],'Salpeter, \Gamma=1.35','Bottom Heavy, \Gamma=2.0','Kroupa IMF (Kroupa et ...
    al. 2001)',...
     'Kroupa01','BH Z0.8','BH Z1.2','Salp Z0.8','Salp Z1.2','Salp SFR Z1','Salp SFR Z0.8','Salp ...
        SFR Z1.2',...
     '-2.0 SFR Z1 ','-2.0 SFR Z0.8','-2.0 SFR Z1.2')

legend1 = legend(gca,'show');
set(legend1,'FontSize',16,'Location','Best');
```

```matlab
set(gca,'YGrid','off',...
    'Yminortick','on',...
    'XMinorTick','on',...
    'XMinorGrid','off',...
    'XGrid','off',...
    'Layer','top',...
    'FontSize',16,...
    'box','on');

%Plot V-IC Color index

figure(3)

hold on

[s20fillvc,msg]=jbfill(log10(age),VIC(:,3)',VIC(:,5)',[0.729411780834198 0.831372559070587 ...
    0.95686274766922],...
    [0.729411780834198 0.831372559070587 0.95686274766922],1,1);
[s13fillvc1,msg]=jbfill(log10(age),VIC(:,5)',VIC(:,6)',[1 0.8 0.8],[1 0.8 0.8],1,1);

hold off

figure(3)
hold on

VIC1=plot(log10(age),VIC(:,1),'Color',[0.749019622802734 0 0.749019622802734],'linewidth',1.5)
VIC2=plot(log10(age),VIC(:,2),'k','linewidth',1.5)
%NGC 4261 4374 4472 3818 1316 1374 1375 1381 1427
VICO=[1.26 1.24 1.23 1.20 1.17 1.20 1.07 1.20 1.15];
VICOE=[0.009 0.008 0.010 0.013 0.032 0.007 0.014 0.012 0.006];
ageic=[12.4 11.8 8.5 5 3.4 7.7 1.5 6.6 7.9].*1e9;
errorbar(log10(ageic),VICO,VICOE,'k+','linewidth',1.5)

Xlim([log10(age(1)) log10(age(end))])
Ylim([-0.8 1.5])
xlabel('log Age','FontSize',16)
ylabel('V-I_C','FontSize',16)
title('a)','FontSize',16)
legend([VIC1 VIC2],'\Gamma=1.35','\Gamma=2.0','-2.0 0.8Z','-2.0 1.2Z','-1.35 0.8Z','-1.35 ...
```

```matlab
    1.2Z','-1.35 1Z sfr',...
    '-1.35 0.8Z sfr','-1.35 1.2Z sfr','-2.0 1Z sfr','-2.0 0.8Z sfr','-2.0 1.2Z sfr')

legend1 = legend(gca,'show');
set(legend1,'FontSize',16,'Location','Best');

set(gca,'YGrid','off',...
    'Yminortick','on',...
    'XMinorTick','on',...
    'XMinorGrid','off',...
    'XGrid','off',...
    'Layer','top',...
    'FontSize',16,...
    'box','on');

figure(4)

hold on

[s20fillvc,msg]=jbfill(log10(age),VIC(:,3)',VIC(:,5)',[0.729411780834198 0.831372559070587 ...
    0.95686274766922],...
    [0.729411780834198 0.831372559070587 0.95686274766922],1,1);
[s13fillvc1,msg]=jbfill(log10(age),VIC(:,5)',VIC(:,6)',[1 0.8 0.8],[1 0.8 0.8],1,1);

hold off

figure(4)
hold on
VIC1=plot(log10(age),VIC(:,1),'Color',[0.749019622802734 0 0.749019622802734],'linewidth',1.5)
VIC2=plot(log10(age),VIC(:,2),'k','linewidth',1.5)
%4261 4374 4472 3818 1316 1374 1375 1381 1427
VICO=[1.26 1.24 1.23 1.20 1.17 1.20 1.07 1.20 1.15];
VICOE=[0.009 0.008 0.010 0.013 0.032 0.007 0.014 0.012 0.006];
ageic=[12.4 11.8 8.5 5 3.4 7.7 1.5 6.6 7.9].*1e9;
errorbar(log10(ageic),VICO,VICOE,'k+','linewidth',1.5)

VIC1=plot(log10(age),VIC(:,1),'Color',[0.749019622802734 0 0.749019622802734],'linewidth',1.5)
VIC2=plot(log10(age),VIC(:,2),'k','linewidth',1.5)
```

```matlab
Xlim([8 10.3])
%Ylim([1.065 1.475])
xlabel('log Age','FontSize',16)
ylabel('V-I_C','FontSize',16)
title('b)','FontSize',16)
legend([VIC1 VIC2],'\Gamma=1.35','\Gamma=2.0','-2.0 0.8Z','-2.0 1.2Z','-1.35 0.8Z','-1.35 ...
    1.2Z','-1.35 1Z sfr',...
    '-1.35 0.8Z sfr','-1.35 1.2Z sfr','-2.0 1Z sfr','-2.0 0.8Z sfr','-2.0 1.2Z sfr')

legend1 = legend(gca,'show');
set(legend1,'FontSize',16,'Location','Best');

set(gca,'YGrid','off',...
    'Yminortick','on',...
    'XMinorTick','on',...
    'XMinorGrid','off',...
    'XGrid','off',...
    'Layer','top',...
    'FontSize',16,...
    'box','on');

figure(5)

hold on

[s20fillvc,msg]=jbfill(log10(age),VIJ(:,3)',VIJ(:,5)',[0.729411780834198 0.831372559070587 ...
    0.95686274766922],...
    [0.729411780834198 0.831372559070587 0.95686274766922],1,1);

[s13fillvc1,msg]=jbfill(log10(age),VIJ(:,5)',VIJ(:,6)',[1 0.8 0.8],[1 0.8 0.8],1,1);

hold off

figure(5)
hold on

VIJ1=plot(log10(age),VIJ(:,1),'Color',[0.749019622802734 0 0.749019622802734],'linewidth',1.5)
VIJ2=plot(log10(age),VIJ(:,2),'k','linewidth',1.5)
%VIC3=plot(log10(age),VIC(:,3),'c','linewidth',1.5)
```

```matlab
%VIC4=plot(log10(age),VIC(:,4),'r','linewidth',1.5)
%VIC5=plot(log10(age),VIC(:,5),'g','linewidth',1.5)
%VIC6=plot(log10(age),VIC(:,6),'b','linewidth',1.5)
%co2=plot(age_co,CO2,'k','linewidth',1.5)
%co3=plot(age_co,CO3,'c','linewidth',1.5)
%co4=plot(age_co,CO4,'g','linewidth',1.5)
%co5=plot(age_co,CO5,'b','linewidth',1.5)
%co6=plot(age_co,CO6,'r','linewidth',1.5)
%%co7=plot(age_co,CO7,'m--','linewidth',1.5)
%co8=plot(age_co,CO8,'m--','linewidth',1.5)
%co9=plot(age_co,CO9,'b--','linewidth',1.5)
%co10=plot(age_co,CO10,'r--','linewidth',1.5)
%co11=plot(age_co,CO11,'k--','linewidth',1.5)
%co12=plot(age_co,CO12,'c--','linewidth',1.5)
%co13=plot(age_co,CO13,'g--','linewidth',1.5)


Xlim([log10(age(1)) log10(age(end))])
Ylim([-0.25 1.8])
xlabel('log Age','FontSize',16)
ylabel('V-IJ','FontSize',16)
title('V-IJ Color index as a function of log age for the different IMFs','FontSize',16)
legend([VIJ1 VIJ2],'-1.35','-2.0','-2.0 0.8Z','-2.0 1.2Z','-1.35 0.8Z','-1.35 1.2Z','-1.35 1Z ...
    sfr',...
    '-1.35 0.8Z sfr','-1.35 1.2Z sfr','-2.0 1Z sfr','-2.0 0.8Z sfr','-2.0 1.2Z sfr')

legend1 = legend(gca,'show');
set(legend1,'FontSize',16,'Location','Best');

set(gca,'YGrid','off',...
    'Yminortick','on',...
    'XMinorTick','on',...
    'XMinorGrid','off',...
    'XGrid','off',...
    'Layer','top',...
    'FontSize',16);

%percentage difference @ 10Gyr
```

```
%VIJ color index
VIJdiff=(VIJ(58,2)-VIJ(58,1))./VIJ(58,1)*100

%VIC color index
VICdiff=(VIC(58,2)-VIC(58,1))./VIC(58,1)*100

%ML ratio
MLdiff=(ML(58,2)-ML(58,1))./ML(58,1)*100
```